

NBSIR 73-334 (R)

A BROADBAND COAXIAL NOISE SOURCE PRELIMINARY INVESTIGATIONS

W. C. Daywitt
L. D. Driver

Electromagnetics Division
Institute for Basic Standards
National Bureau of Standards
Boulder, Colorado 80302

October 1973

Interim Status Report
Contract No. CCG/Navy Blanket
Program 73-78

Prepared for
Department of Defense
Calibration Coordination Group
Attn: Melvin L. Fruechtenicht, Chairman
Army Metrology and Calibration Center
Redstone Arsenal
Huntsville, Alabama 35809
CCG 73-78

NBSIR 73-334

A BROADBAND COAXIAL NOISE SOURCE PRELIMINARY INVESTIGATIONS

W. C. Daywitt
L. D. Driver

Electromagnetics Division
Institute for Basic Standards
National Bureau of Standards
Boulder, Colorado 80302

October 1973

Interim Status Report
Contract No. CCG/Navy Blanket
Program 73-78

Prepared for
Department of Defense
Calibration Coordination Group
Attn: Melvin L. Fruechtenicht, Chairman
Army Metrology and Calibration Center
Redstone Arsenal
Huntsville, Alabama 35809
CCG 73-78



U.S. DEPARTMENT OF COMMERCE, Frederick B. Dent, Secretary

NATIONAL BUREAU OF STANDARDS, Richard W. Roberts, Director

CONTENTS

	<u>Page</u>
INTRODUCTION-----	1
1. NOISE TEMPERATURE APPROXIMATION FOR A COAXIAL NOISE STANDARD-----	4
2. RESONANCE TECHNIQUE (TE01 CIRCULAR MODE) FOR MEASURING DIELECTRIC CONSTANT VS. TEMPERATURE-----	6
3. BROADBAND BEAD DESIGN-----	10
4. BROADBAND TERMINATION DESIGN-----	24
5. FIGURES-----	29
6. APPENDICES	
A. CCG Work Statement-----	48
B. Output Noise Temperature for a Coaxial Noise Source---	52
C. Propagation Constant of a Coaxial Line-----	58
D. Design Formula for the TE01 Circular Mode Resonance Measurement-----	61
E. Propagation Constant in a Lossy Dielectric-----	64
F. Dielectric Constant Measurement Using the Automatic Network Analyzer-----	66
G. Curve Fitting Equation for Bead and Line Trimming-----	71
H. Step Capacitance-----	76
I. Effective Dielectric Constant and Face Compensation-----	77
J. Higher Mode Bead Resonances-----	82

CONTENTS (Continued)

	<u>Page</u>
K. TE11 Cutoff Wavelengths-----	85
L. Termination Design Equations-----	86
7. REFERENCES-----	87

LIST OF FIGURES

Figure 1. TE01 Circular Mode Dielectric Measurement System-----	30
Figure 2. D·F Graph for TE01 Measurement-----	31
Figure 3. Table of TE01 Measurements for Various Materials-----	32
Figure 4. Bead Resonant Frequencies for TE11 Circular Mode in 14 mm Bead-----	33
Figure 5. Measurement Data for 14 mm Bead-Line Before Compensation-----	34
Figure 6. 14 mm Bead and Line-----	35
Figure 7. Measurement Data for 14 mm Bead-Line After Compensation-----	36
Figure 8. 7 mm Bead and Line-----	37
Figure 9. Measurement Data for 7 mm Bead-Line Before Compensation-----	38
Figure 10. Measurement Data for 14 mm Bead-Line-Gap Before Compensation-----	39
Figure 11. Measurement Data for 14 mm Bead-Line-Gap After Compensation-----	40
Figure 12. Resistive Cone and Cone Holder for 7 mm Termination-----	41
Figure 13. Resistive Cone-----	42
Figure 14. Cone Holder-----	43

LIST OF FIGURES (Continued)

	<u>Page</u>
Figure 15. Equivalent Circuit for Derivation of Equation G.11-----	44
Figure 16. Profile View and Equivalent Circuit for Derivation of Equation I.11-----	45
Figure 17. Profile View for Derivation of Equation J.6-----	46
Figure 18. Graph of $(1 + k)X'_{11}$ -----	47

ABSTRACT

This report describes investigations that were performed in fiscal year 1973, by the Noise and Interference Section of the Electromagnetics Division of the Institute for Basic Standards of the National Bureau of Standards preliminary to the design and construction of a coaxial thermal noise source in fiscal year 1974. The intent is to develop a coaxial thermal reference noise source that will operate at nominally 1000°C and will have a low reflection coefficient from 0.1 to 12 GHz.

Key words: Bead support; noise standard; resistive termination.

A BROADBAND COAXIAL NOISE SOURCE

Preliminary Investigations

INTRODUCTION

This report is a report to sponsor of a number of investigations that were performed during fiscal year 1973 in preparation for the design and construction of a coaxial thermal reference noise standard. The sponsor is the Calibration Coordination Group of the Department of Defense, and the task is designated by either number CCG 73-78 or NBS 2726449. The proposed noise standard is to have the following specifications:

- (1) Noise temperature output is to be nominally
1273 K.
- (2) Broadband characteristics require as low a reflection
coefficient as possible from 0.1 to 12 GHz.

In order to design and build this high temperature, broadband noise standard four things are needed: 1) a method for calculating the noise temperature of the coaxial noise source; 2) an accurate method of measuring the dielectric constant of candidate inner conductor bead support materials usable at elevated temperatures; 3) a means for designing broadband bead supports for the inner conductor; and 4) a broadband termination design that will withstand usage at elevated temperatures.

In essence this year's work has been aimed at developing needed techniques and know how to accomplish the above. The following tasks emerged as the most critical for the success of these objectives:

- (1) to develop a technique for measuring dielectric constant at high temperatures;
- (2) to develop a predictable technique for designing low reflection bead supports for the center conductor of the noise source;
- (3) to investigate and select the most workable thin-film termination design;
- (4) experiment to find a means for retaining a thin-film on a ceramic substrate at or near 1000°C ;
- (5) to try to develop a technique for adjusting the termination for a low reflection coefficient.

These tasks can be recognized as being mainly concerned with achieving a low reflection coefficient at high temperatures for the termination and transmission line. For comparison the original CCG work statement is included in its entirety as Appendix A.

Section one of this report describes a method for calculating the noise temperature output of a coaxial thermal noise source.

The first of the preceding five tasks has been completed and is discussed in section 2.

Task number two is 90% complete but was discontinued in this fiscal year for lack of funds. It appears that about three weeks of the next fiscal year effort will be needed for its completion. This task is discussed in section 3.

Task number three is tentatively complete with the choice of a conical termination design as discussed in section 4.

Task number four is approximately 50% complete and will be continued into the next fiscal year. It is discussed in section 4.

Task number five was not started in order to allow sufficient funds for task four and for writing this report. Some comments concerning this task will be found in section 4 however.

From the above it is apparent that task 2 was not completed, and that task 5 was not begun because of insufficient funds. Sixty thousand dollars was estimated to be needed to accomplish this year's work. Fifty-five thousand dollars were received, and it is estimated now that an additional six thousand dollars would have helped complete tasks two and five.

1. NOISE TEMPERATURE APPROXIMATION FOR A COAXIAL NOISE STANDARD

An accurate calculation of the noise temperature from a waveguide⁽¹⁾ and a coaxial thermal noise standard differs in one important aspect. In a waveguide standard a single temperature distribution along the length of the waveguide is used. The coaxial standard in general has two such distributions, one for the inner and one for the outer conductor. It is this difference that prevents the direct use of previously developed equations for the calculation of the noise temperature.

Equation (1.1) is the formula used to calculate the noise temperature of a rectangular waveguide thermal noise source (Appendix B).

$$T = T_m \alpha_0 + \int_0^l T_x \alpha'_x dx \quad (1.1)$$

The quantity $T_m \alpha_0$ is the contribution to T from the termination, and the integral term is the contribution from the waveguide itself. Clearly the waveguide contribution depends on only one temperature distribution T_x along its length. This term can be rewritten as

$$\int_0^l T_x \alpha'_x dx = 2 \int_0^l \left(\frac{1 + |T_x|^2}{1 - |T_x|^2} \right) T_x u_x dx \quad (1.2)$$

where u_x is the real part of the propagation constant for the elemental length dx of line at position x along the waveguide and α_x is defined in Appendix B. It is significant that T_x and u_x appear as a product.

In a coaxial noise source there are two temperatures associated with each point along the transmission line, one for the outer conductor and one for the inner conductor. However, U_x does not allow a separate identification of inner and outer conductor losses for the TEM wave. That is, U_x does not separate into the sum of two terms, one being solely identified with the outer conductor and one with the inner conductor. Without this separation the outer and inner conductor temperatures cannot be uniquely coupled with the outer and inner conductor losses respectively. Therefore the noise temperature of a coaxial thermal noise source cannot be calculated exactly. However, for low loss lines an approximate separation of U_x is possible and a first order approximation to the noise temperature is obtained. This approximation is developed in Appendices B and C, and it is shown there (Appendix B) that the resulting error in the noise temperature from using this approximation is negligible.

The result of this first order approximation for the noise temperature is given by equation B.9 of Appendix B.

$$T = T_m \alpha_0 + 2 \int_0^L (T_{xi} U_{xi} + T_{xo} U_{xo}) \left(\frac{1 + |T_x|^2}{1 - |T_x|^2} \right) \alpha_x dx \quad (1.3)$$

where T_{xi} and T_{xo} are the temperature distributions for the inner and outer conductors respectively, and U_{xi} and U_{xo} are the first order separated real "propagation constants" for the inner and outer conductors respectively.

This result (eq 1.3) will be used to calculate the output noise temperature of the thermal noise source and will be the basis for developing an error analysis of the coaxial standard.

2. RESONANCE TECHNIQUE (TE01 CIRCULAR MODE) FOR MEASURING DIELECTRIC CONSTANT vs. TEMPERATURE

In the design, testing, and troubleshooting of the coaxial noise standard it will be necessary to identify and isolate reflections from a number of sources. One source of reflection is an impedance mismatch between the transmission line and the bead support(s) for the inner conductor. To minimize this mismatch in the initial design of the bead support(s) an accurate (i.e., $\pm 5\%$ or better) measurement of the dielectric constant of the bead material is required at the working temperature. To this end the TE01 circular mode resonance technique⁽²⁾ was implemented, based on a brief survey of candidate methods for measurements up to 1000°C .

The technique (Appendix D) involves resonating the TE01 circular waveguide mode in a cylindrical dielectric sample that has been fitted into a uniform diameter hollow cylindrical tube. The resonant frequency satisfies the requirement that the TE01 mode propagates inside the sample but is cut off outside of the sample. Since the electric field in the sample vanishes at the inner surface of the tube, for this mode, a small air gap between the sample and pipe does not greatly affect the dielectric constant measurement.⁽²⁾ This lack of sensitivity to such gaps allows the sample to be heated with negligible error due to the gap produced by the heating.

The simplicity of the system can be explained with the aid of figure 1. RF energy is fed from the sweep generator into the coax-to-waveguide adaptor at the right end of the X-band waveguide structure. The rf energy proceeds through the isolated reaction cavity and directional coupler to a waveguide-to-3mm coaxial adaptor. The rf energy is coupled to the sample residing in the circular tube through a small magnetic probe at the end of the 3mm coaxial line. The reflected energy travels back through the 3mm line, through the adaptor and up the vertical arm of the directional coupler to the tunable crystal detector. The detected signal is fed into the vertical display of the oscilloscope whose horizontal axis is being swept by the sweep output of the sweep generator. The oscilloscope display shows two resonances. The right one in figure 1 is the sample resonance and the left one is the resonance from the reaction cavity that is shown for comparison. The sample material whose resonance is being displayed is an isotropic pyrolytic boron nitride. A number of tubes and samples used during these preliminary investigations are shown under and to the left of the tube being used.

When a dielectric constant is to be measured at a high temperature a tube of high temperature metal containing the sample will be placed in an oven at the desired temperature. In this case a high temperature 3mm coaxial line will be used to excite the sample. This high temperature line is shown in the center of the figure leaning against the waveguide rail.

This technique requires that the product of the tube diameter D and the resonant frequency f must lie between the values shown in figure 2. Then if the approximate value of the relative dielectric constant ϵ_r (Appendix F) is known at the desired frequency an accurate value of ϵ_r at the same frequency can be obtained by adjusting the sample length and diameter with the aid of figure 2 and equations D.2 and D.3 of Appendix D.

To test the theory and the system a number of samples were measured and compared to measurements made using a slotted line technique⁽³⁾ that was adapted to measure ϵ_r at any given frequency.⁽⁴⁾ Figure 3 shows the results of these tests using two batches of boron nitride as the sample material. In the first column Cu or Al indicate resonance measurements in which a copper or aluminum tube was used for the circular waveguide. "Coax" indicates that the measurement was performed with the slotted line technique. The sample batch number indicates from which boron-nitride batch the sample was cut. The frequencies given in the sixth column are the measured resonance frequencies, or the frequencies at which the measurements were performed with the slotted-line technique.

By examining figure 3 the following conclusions and implications can be drawn:

- (1) Both the sets (coax and resonance measurements) have a high internal consistency. For example, the relative spreads in the value of ϵ_r measured by the resonance (1-6) and coax techniques (7, 8) about their average values are 0.24% and 0.07% respectively.

(2) Although both sets of measurements are repeatable to a fraction of a percent, they nevertheless differ by approximately 3% as evidenced by the average values of 4.632 and 4.490 measured via the resonance and coax techniques respectively.

(3) In the resonance measurements an air-gap does have a negligible effect on the measured values as evidenced from the small differences between the separate values and the average value of 4.632 for the resonance measurements.

(4) Since the measurements using the Cu and Al tubes give essentially the same results, the wall losses of the tubes have a negligible effect on the measured dielectric constant.

(5) A number of resonance measurements not appearing in this table were made with different sample loadings (different separation distances between the rf probe and the sample face) that indicate the results obtained to be free from excessive coupling.

The preceding results imply that the resonance technique is capable of measuring dielectric constants at elevated temperatures quite precisely although there is some question about the accuracy. Since there is a 3% difference between the coax and resonance measurements, a maximum error of 3% in the resonance technique will be assumed. This assumed error is not crucial to the concerns of this report, but does allow some order-of-magnitude

estimates to be made in section 3 under the "Formula Test Results."

Due to the non-crucial nature of the assumed error no extensive effort was used to track down the source of the discrepancy between the resonance and coax values for ϵ_r .

Once the final bead material or materials are chosen a high temperature tube or tubes of appropriate dimension will be purchased and the dielectric versus temperature measurements performed. At present not enough is known concerning the final design to allow this choice.

Another technique was partially investigated that may prove useful if it becomes necessary to measure dielectric constant versus frequency. This technique (Appendix F) utilizes an automatic network analyzer to measure the scattering coefficients of a two-port comprised of a coaxial reference air line filled with the dielectric material under question. From these measured scattering coefficients the analyzer calculates and prints out the dielectric constants for the frequencies of interest. This technique doesn't have a high degree of accuracy, but could nevertheless be used to confirm or eliminate the question of anomalous dielectric constant behavior should it arise.

3. BROADBAND BEAD DESIGN

The principal mode characteristic impedance Z_0 of a coaxial transmission line is given by equations 3.1 or 3.2

$$Z_o = \frac{1}{2\pi} \left(\frac{\mu_o}{\epsilon_o} \right)^{1/2} \frac{1}{\epsilon_r^{1/2}} \ln \frac{D_o}{D_i} \quad (3.1)$$

$$\approx \frac{60}{\epsilon_r^{1/2}} \ln \frac{D_o}{D_i}$$

$$Z_o = \left(\frac{L}{C} \right)^{1/2} \quad (3.2)$$

where μ_o and ϵ_o are the free space magnetic and electric permittivities respectively, ϵ_r is the relative dielectric constant of the material filling the line, D_o is the inner diameter of the outer conductor and D_i is the outer diameter of the inner conductor, and L and C are the inductance and capacitance per unit length respectively of the line. In constructing a transmission line using bead supports for the inner conductor, Z_o must be the same for each point along the length of line if the line is to be broadband, that is if the line is to have no reflections. ⁽⁵⁾ For example, in the air filled region of a 50 ohm line the diameter ratio D_o/D_i in equation (3.1) must be chosen to make Z_o equal to 50 ohms with ϵ_r equal to unity. However, within the bead supports whose relative dielectric constant might be 4 this ratio must be chosen to make Z_o equal to 50 ohms with ϵ_r equal to 4. Therefore, at the interfaces between the bead supports and the air the diameters of the inner and outer conductors are abruptly changed to maintain the 50 ohm characteristic impedance. This abrupt change or step in the conductors produces an anomalous increase in the capacitance of the line at the step through the resulting fringing fields. ⁽⁶⁾

This step capacitance leads to a reflection since C in equation (3.2) is increased by the step capacitance at the step and the resulting Z_0 is less than the desired 50 ohms. In order to decrease C back to the correct value to make Z_0 50 ohms, some of the capacitance at the step is removed by removing some of the material from the bead faces. This is usually accomplished by cutting a shallow toroidal groove in the bead faces concentric with the conductors. (6)

If the above is properly done, the line and bead supports will be reflectionless from dc up to the lowest frequency at which the higher modes begin to propagate within the bead, and it is therefore desirable to have a formula for predicting the lowest frequency for the onset of these modes.

3.1 Bead Support Design and Trimming

The design, construction, and subsequent trimming of bead supports to make them reflectionless is accomplished by the following procedure:

1. An accurate measurement (see Sec. 2) of the dielectric constant of the bead material is obtained.
2. Equation (3.1) is used to determine the correct diameter ratio for the conductors in the region of the bead support so that this region will have the correct characteristic impedance, Z_0 , for the relative dielectric constant ϵ_r of the material measured in step 1.
3. An upper limit to the length of the bead is obtained from the graph of the equation (J.6) in Appendix J (Fig. 4). This equation gives the frequencies at which the bead acts as a cavity at resonance for

the odd and even configurations of the TE₁₁ circular waveguide mode. The odd and even configurations appear alternately as the frequency is increased, the first resonance to appear being that of the even configuration. The details of this equation are explained in Appendix J.

4. The diameter of the outer conductor is increased and/or the diameter of the inner conductor is decreased where the bead is to be placed in accordance with the value of D_o/D_i calculated in step 2. This increase and/or decrease in the diameters is not fully completed, however, allowing for some inaccuracy in the measurement of ϵ_r . Later reflection measurements will indicate how much conductor trimming is left to be done. The length of the bead and the changed diameter portions of the line are determined in accordance with step 3, and a bead is cut to press fit into the enlarged line.

A graph of equation (J.6) for the first even and odd modes is shown in figure 4 for a 14 mm line and bead. The resonant frequencies for these modes are plotted horizontally for the bead lengths plotted vertically. For example, for a 2 cm bead with a dielectric constant equal to 4.56 with the dimensions given in the graph, the first resonance occurs at about 5.4 GHz. The next resonance to appear will be at about 6.8 GHz and is due to the first appearance of the odd mode. As the frequency is increased an infinite sequence of resonance frequencies

are encountered. The cutoff frequency for these TE₁₁ modes is 4.86 GHz for the dielectric constant in the figure and is a vertical asymptote for all the modes.

The actual bead length is then chosen to be less than that length where the first even mode appears for the highest frequency at which the bead and transmission line are to be used. For example, if the bead and line of figure 4 is to be used up to 9 GHz, the bead length should be no greater than 0.1 cm where the first even configuration appears. After the bead is compensated for the step capacitance it resonates at a frequency given by its original length minus the length removed. For example, if 0.2 cm were cut into each face of the 2 cm bead, its resonant length would be reduced to 1.6 cm and the corresponding first resonant frequency would be increased from 5.4 GHz to about 5.5 GHz.

5. The reflection coefficient magnitude (equation 3.3 below) of the bead and line is measured as a function of frequency on the automatic network analyzer, the data is plotted, and the constants \mathcal{D}_1 and \mathcal{D}_2 are determined. The resulting plot of such a measurement is shown in figure 5, where the dots represent measured data points. The abscissa is the measurement frequency in gigahertz and the ordinate is the reflection coefficient. The angles given under the major frequency divisions are the electrical angles $(2\pi f / f_0)$

corresponding to the given frequency, where f_0 corresponds to a full cycle or 360° . For example, 90° corresponds to 4.84 GHz and is that point where only the first term or D_1 is present from equation (3.3). The constants D_1 and D_2 of equation (3.3) for the reflection coefficient (see Appendix G for a derivation of this equation) are then chosen to make the equation fit the data points.

$$|T| = \left| D_1 \sin \frac{2\pi f}{f_0} - \frac{D_2 f}{f_0} \cos \frac{2\pi f}{f_0} \right| \quad (3.3)$$

where f_0 is that frequency for which the electrical length of the bead is one wavelength, and f is the measurement frequency. This equation is a first order equation in D_1 and $D_2 f / f_0$. D_1 is the reflection coefficient caused by the characteristic impedance of the bead being different from 50Ω , and D_2 is the reflection coefficient caused by the step capacitance.

A nonvanishing D_1 indicates that the diameter ratio in equation (3.1) was not properly chosen for the given dielectric constant of the bead. If the outer conductor diameter b' in the bead region is too large by $\delta b'$, and/or if the inner conductor diameter a' in the bead region is too large by $\delta a'$, and/or if ϵ_r is too large by $\delta \epsilon_r$, then the resulting reflection D_1 is related to $\delta b'$, $\delta a'$, and $\delta \epsilon_r$ by (see Appendix G for details)

$$D_1 = \frac{6}{5\epsilon_r^{1/2}} \left(\frac{\delta b'}{b'} - \frac{\delta a'}{a'} \right) - \frac{1}{2} \frac{\delta \epsilon_r}{\epsilon_r} \quad (3.4)$$

In using equation (3.4) to determine what correction to the conductor diameters or ϵ_r is needed to make D_1 vanish, either $\delta \epsilon'$, $\delta a'$, or $\delta \epsilon_r$, or any two of these can be taken as zero and the correction made entirely on only one of them.

Before any compensation of the bead for the reflection caused by the step capacitance is made D_2 will be nonvanishing. D_2 is related to the step capacitance C (see Appendix I) through the relation

$$D_2 = (D_2)_0 (1 - d/d_0) \quad (3.5)$$

where

$$(D_2)_0 = 2\pi f_0 Z_0 C \quad (3.6)$$

$(D_2)_0$ is the value of D_2 before any compensating cuts ($d=0$) are made into the bead faces, d is the cutting depth, and d_0 is that depth of cut which perfectly nullifies ($D_2=0$) the reflection from the step capacitance.

A rough estimate of d_0 (see Appendix I) is given by

$$d_0 = \frac{Z_{02} l (D_2)_0}{2\pi (Z_{02}^2 - 1)} \quad (3.7)$$

where

$$Z_{02}^2 = \epsilon_r / \epsilon_{re} \quad (3.8)$$

ϵ_{re} (see Appendix I) is the effective relative dielectric constant in the portions of the bead where the compensating toroidal cuts have been made, and ℓ is the bead length. Since this first measurement is made before any bead compensating is done ($d=0$), the value of D_2 determined is the same as $(D_2)_0$.

Equation (3.7) is now used to determine what approximate depth of compensation of the bead will cancel the reflection from the step capacitance.

6. After d_0 is determined from step 5, a toroidal cut is made into both faces of the bead to a depth that is some fraction of d_0 (e.g. 1/2 or 1/3), and another set of reflection measurements is made and plotted. Again D_1 and D_2 are determined from the graph. If D_1 agrees with the previous D_1 measured in step 5, it is safe to change the conductor diameters accordingly in the region of the bead. If not, then enough care was not taken in fitting the bead in the line and the process in the previous steps should be repeated until agreement is obtained. Great care must be exercised in the machining and fitting of the line and bead if the value measured for D_1 is to be meaningful. The second measured value of D_2 should show some agreement with equation (3.5).

7. Steps 5 and 6 are repeated until the bead-line reflection coefficient is reduced to or below the desired value.

Formula Test Results

This first set of results is meant to show that the preceding formula and ideas have sufficient validity to be gainfully used in the design and construction of broadband bead supports.

The first group of results pertain to figures 4, 5, 6, and 7. Figure 6 is an exploded view of the 14 mm bead-line test apparatus, consisting of an air line whose diameters have been changed in the bead region. The bead is made of boron nitride and is fitted onto the center conductor. A compensation groove can be seen in the visible face of the bead. Figure 4 has been discussed and is used to predict the bead resonant frequencies for the 14 mm bead and line. Before any compensation was performed the predicted resonant frequency corresponding to the bead length of 0.725 cm was approximately 6.4 GHz. This prediction compares well with the measured resonant frequency of 6.7 GHz indicated in figure 5. After a 0.152 cm compensation cut was made into both faces the effective length of the bead was reduced from 0.725 cm to 0.421 cm. The predicted resonant frequency corresponding to this length is 7.2 GHz as obtained from figure 4. This value compares well with the measured value of 7.6 GHz as shown in figure 7. The broad spike at 5.8 GHz in figure 7 is believed to be generated in the network analyzer and is not a resonance. This coupled with further experiments indicates that equation (J.6) of Appendix J is quite adequate for predicting the onset frequency for bead resonances, at least for 14 mm and 7 mm lines with bead supports of moderate dielectric constant.

The calculation of the step capacitance of the 14 mm bead before compensation using equation (H.1) of Appendix H gave 0.21 picofarads for C . The measured value obtained from $(D_z)_0$ through equation (3.6) was 0.22 picofarads, in good agreement with the calculated value. The second order value of 1.35 for D_z was used in equation (3.6) although the first order value, that obtained from equation (3.3), would also have given good agreement. The second order value was obtained using a second order equation for $|V|$ analogous to the first order equation given by (3.3). This was done to better understand the data points and equation (3.3), and to get a better expression for determining the value of the step capacitance for $d=d_0$, and consequently the relationship (I.9) in Appendix I. According to equation (3.3) the data points in figure 5 should pass through zero at 4.84 GHz. The fact that they do not is due to the first order nature of equation (3.3).

From figure 5 and the value of 1.35 for D_z the depth of compensation cut needed to nullify the reflection from the step capacitance is 0.153 cm as calculated from equation (3.7). After a cut of 0.152 cm was made into each face the resulting D_z is + 0.0071 as seen in figure 7. The corresponding D_z calculated from equation (3.5) is + 0.009 in good agreement with the measured value.

The value of D_1 obtained from figure 5 is approximately zero, showing that the diameter ratio in equation (3.1) is apparently close to correct

for the value of ϵ_r measured for the bead. However, the value calculated from equation (3.4) is -0.046 , taking $\delta\alpha'$ and $\delta\epsilon_r$ to be zero. The value obtained from figure 7 for D_1 is -0.045 in close agreement with the calculated value of -0.046 . D_1 should be the same for both figures 5 and 7. The discrepancy implied by $D_1 \approx 0$ from figure 5 can only mean therefore that $-\delta\epsilon_r/2\epsilon_r$ in equation (3.4) must have been approximately equal to $+0.046$ to offset the first term in equation (3.4), giving approximately zero for D_1 . The only way this could have happened is for $\delta\epsilon_r/\epsilon_r$ to be approximately -9.2% , a number three times larger than the maximum measurement error of 3% for ϵ_r assumed in section 2. This leads to the conclusion that the outer diameter of the bead used for figure 5 was undersized and that the bead used for figure 7 was a good fit. This was indeed the case, and it points up the extreme care needed in fitting the bead into the line.

Figure 8 shows an exploded view of the 7 mm bead holder that was constructed to further test the design formula. The bead is made from boron nitride, and with the line is dimensioned such that at least two bead resonances will appear in the 0 to 12 GHz frequency range. This picture was taken after the bead had been partially compensated and the groove can be seen around the center conductor of the line. The reflection coefficient measured on the automatic network analyzer for this line and bead before the bead was compensated is plotted as a function of frequency in figure 9. Again the isolated

points represent the measured data and the solid curve represents the best fit for equation (3.3). At around 4.5 GHz the curve and data points begin to diverge possibly owing to the first order nature of equation (3.3). The sudden jump in the data points at 9.5 GHz is apparently due to the measurement apparatus since this jump is not explainable by the bead reflections or resonances. The value for \mathcal{D}_2 implies a step capacitance of 0.26 picofarads, while the value calculated from equation (H.1) is 0.29 picofarads. Using equation (3.4), the value of \mathcal{D}_1 indicates that the diameter of the outer conductor is too small by 18% $\left(0.1 \times 5 \times \epsilon_r^{1/2} / 6\right)$, or that the diameter of the inner conductor is too large by 18%, or that ϵ_r is too large by 20%. If the value for \mathcal{D}_1 is correct it indicates that the conductors should be changed accordingly to reduce \mathcal{D}_1 to zero, or in this case since $\delta\epsilon_r$ is positive, ϵ_r could be reduced to some effective value (Appendix I) 20% lower than its present value to accomplish the same end. The ability to tune the bead by lowering its dielectric constant through removing some of the bead material the whole length of the bead should prove quite useful later on in the standard's development. Two resonant frequencies in the 0 - 12 GHz range are predicted for the bead by equation (J.6) in Appendix J, the lower resonant being that of the first even mode and the second being that of the first odd mode. The values predicted for these resonant frequencies are 5.5 GHz and 8.3 GHz, both of which are 14% lower than the measured values of 6.4 GHz and 9.6 GHz.

Gap Experiment Results

Even if a bead and line are press fit together, when they are both heated a small gap may appear between one of the outer conductors and the bead. This gap will both change the bead characteristic impedance and its step capacitance, causing the reflection coefficient to increase. The work of Cruz⁽⁷⁾ with effective dielectric constants implies that this gap problem can be circumvented by inserting ϵ_{re} in place of ϵ_r in the design and trimming formula, where ϵ_{re} is less than ϵ_r and accounts for the gap. The expression for ϵ_{re} in this case can be obtained from equation (I.2) of Appendix I by using equation (I.1) and letting b'' equal b' , and a'' equal the reduced bead outer diameter $b'-2g$ where g is the gap width. Then

$$\epsilon_{re} = \frac{\epsilon_r}{1 + (\epsilon_r - 1) \ln(b'/(b'-2g)) / \ln(b'/a')} \quad (3.9)$$

Although in reality the gap will not be concentric with the conductors, it is expected that the eccentricity is a second or higher order effect and that this treatment of the gap problem will still be useful. The experiment to be described now supports this conclusion. It consists of constructing a bead whose outer diameter is 5 mils (0.013 cm) smaller than the outer line diameter of the 14 mm line. In other words the bead and line are the same as in figure 6 with the bead reduced by 5 mils in its outer diameter. The reflection coefficient

of the bead and line is then measured before and after compensation and the measurement results compared with those predicted by equations (3.3), (3.6), and (3.7), and equation (H.1) of Appendix H.

Figure 10 shows the measurement results before compensation. The best fit for $|\Gamma|$ is given by -0.033 and $+0.859$ for \mathcal{D}_1 and \mathcal{D}_2 respectively. Equation (3.6) and the measured value of \mathcal{D}_2 lead to a value of 0.14 picofarads for the step capacitance C . The value obtained for C from equation (H.1) is 0.19 picofarads which compares favorably with the measured value. The depth \mathcal{L}_0 of cut to provide full compensation calculated from equation (3.7) and equation (I.2) is 0.097 cm. The predicted TE₁₁ resonant frequency using equation (J.6) of Appendix J is 6.4 GHz compared to a measured value of 6.9 GHz. The range of values obtained for \mathcal{D}_1 is -0.08 to -0.04 using equation (3.4) with ϵ_{re} of equation (3.9) replacing ϵ_r to account for the gap. The measured value for \mathcal{D}_1 before and after compensation is -0.033 in good agreement with the calculated range of values for \mathcal{D}_1 .

Figure 11 shows the measured reflection coefficient of the bead with a 5 mil gap after a compensation cut to a 0.048 cm depth had been made. In this case the bead length for the TE₁₁ resonance calculation is reduced by 0.096 cm giving a resonant frequency of 6.6 GHz as compared to the measured value of 7.1 GHz. \mathcal{D}_1 is the same, -0.033 , as in figure 10 as it should be since no changes to the bead or line diameters have been made. The new measured value for \mathcal{D}_2 is 0.431 . The value calculated for \mathcal{D}_2

using equation (3.5) with $d_0=0.097$, $d=0.048$, and $(D_2)_0=0.959$ is 0.434 which closely agrees with the measured value.

These results show that it is possible to trim a bead and line to achieve a low reflection coefficient even though a gap is present. Although the gap chosen for these measurements was between the outer diameters of the bead and line, these results imply that the same trimming procedure applies to a gap between the bead and line inner diameters.

As a bead and line are heated a gap may also appear between the bead faces and the inner and outer conductor steps next to these faces. This gap will modify the step capacitances which, hopefully, can still be accounted for in the same manner indicated in equation (3.4). However, for lack of time no experiments were conducted to test this statement.

4. BROADBAND TERMINATION DESIGN

Resistive Element Selection

In selecting an appropriate resistive terminating configuration, several different types were considered. Among these were various thin film configurations such as the cylindrical center element with a tractorial outer conductor, the conical center element with a cylindrical outer conductor and several strip line element types^(5, 8, 9). Also, the solid lossy element types were considered.

The conical center element of figure 12 was selected because of the simplicity of design, ease of machining and greater predictability. Also, another group in Division 272 has had considerable past experience with this type of terminating element.

Materials Selection

The 12 GHz upper frequency limit and especially the 1000°C operating temperature place very severe requirements on the materials to be used in the terminating element. The conical substrate and the metallic resistive film must maintain their mechanical and electrical properties up to these limits as well as remain chemically and mechanically compatible with one another.

A literature search for high temperature materials narrowed the choices of suitable substrate materials to a very few. Certain types of boron nitride and beryllium oxide appeared to have very good mechanical and electrical characteristics over the ranges of temperature and frequency of interest. Sapphire, alumina, quartz and silica also seemed to be possible candidates. Samples of pyrolytic isotropic boron nitride, hot pressed boron nitride and beryllium oxide were obtained for initial testing.

Some materials considered as possibilities for the resistive thin film were platinum, rhodium, titanium, tantalum and tungsten. For the first attempt, an alloy of 90% platinum and 10% rhodium was selected. This material was selected because of high melting point, the excellent chemical properties at high temperatures and the vast amount of published

material dealing with the mechanical and electrical characteristics of this alloy. Also, this material has been used in previous high temperature applications with good success. ⁽¹⁾

High Temperature Materials Testing

Several samples each of pyrolytic isotropic boron nitride, hot pressed boron nitride and beryllium oxide were sent out to a local firm for deposition of thin films of the 90% platinum 10% rhodium alloy. The film on each sample was deposited to produce approximately 30 ohms per square.

One sample of each type was subjected to 1000°C for several hours. All three samples failed. Severe surface glazing was experienced with both types of boron nitride. This glazing is believed to result from water absorption by the material prior to film deposition. It has since been observed at temperatures as low as 700°C. The beryllium oxide sample appeared to withstand the temperature but resistance measurements of the film revealed that it had become non-conductive.

Boron nitride as a substrate material has been, at least, temporarily set aside in favor of beryllium oxide. Samples of BeO with the Pt-Rh alloy film have been run in an argon atmosphere and in a vacuum furnace in an effort to determine the cause of the film failure at 1000°C. In all tests the film failed in less than one hour when run at 1000°C. Also, the failure takes place somewhere between 900°C and 1000°C. Samples have been run at 900°C for several days without any sign of change or failure of either the resistive film or the BeO substrate.

Gold was deposited on two samples of BeO and tested at 900°C and 1000°C . These films failed also by becoming non-conductive. However, since several hours were required at 1000°C and two days at 900°C , it is suspected that these failures resulted from sublimation.

Resistive Element Design

Design equations for the tapered conical load are described in Appendix L. A computer program utilizing these equations has been written to calculate the various dimensional requirements (figure 12) for conical substrates of different dielectric constants and for different coaxial line sizes. The program was used to design a 7 mm conical termination to be used at room temperature to gain insight into the characteristics of this type of termination. This termination and its associated housing are shown in figures 13 and 14, respectively.

The authors gratefully acknowledge help from the following persons:
Dr. Howard E. Bussey, W. J. Foote, P. E. Werner, and other personnel
from Section .55 who helped with the use of the Automatic Network Analyzer.

5 . FIGURES

1. TE01 Circular Mode Dielectric Measurement System
2. D•F Graph for TE01 Measurement
3. Table of TE01 Measurements for Various Materials
4. Bead Resonant Frequencies for TE11 Circular Mode in 14 mm Bead
5. Measurement Data for 14 mm Bead-Line Before Compensation
6. 14 mm Bead and Line
7. Measurement Data for 14 mm Bead-Line After Compensation
8. 7 mm Bead and Line
9. Measurement Data for 7 mm Bead-Line Before Compensation
10. Measurement Data for 14 mm Bead-Line-Gap Before Compensation
11. Measurement Data for 14 mm Bead-Line-Gap After Compensation
12. Resistive Cone and Cone Holder for 7 mm Termination
13. Resistive Cone
14. Cone Holder
15. Equivalent Circuit for Derivation of Equation G.11
16. Profile View and Equivalent Circuit for Derivation of Equation I.11
17. Profile View for Derivation of Equation J.6
18. Graph of $(1 + k)X'_{11}$

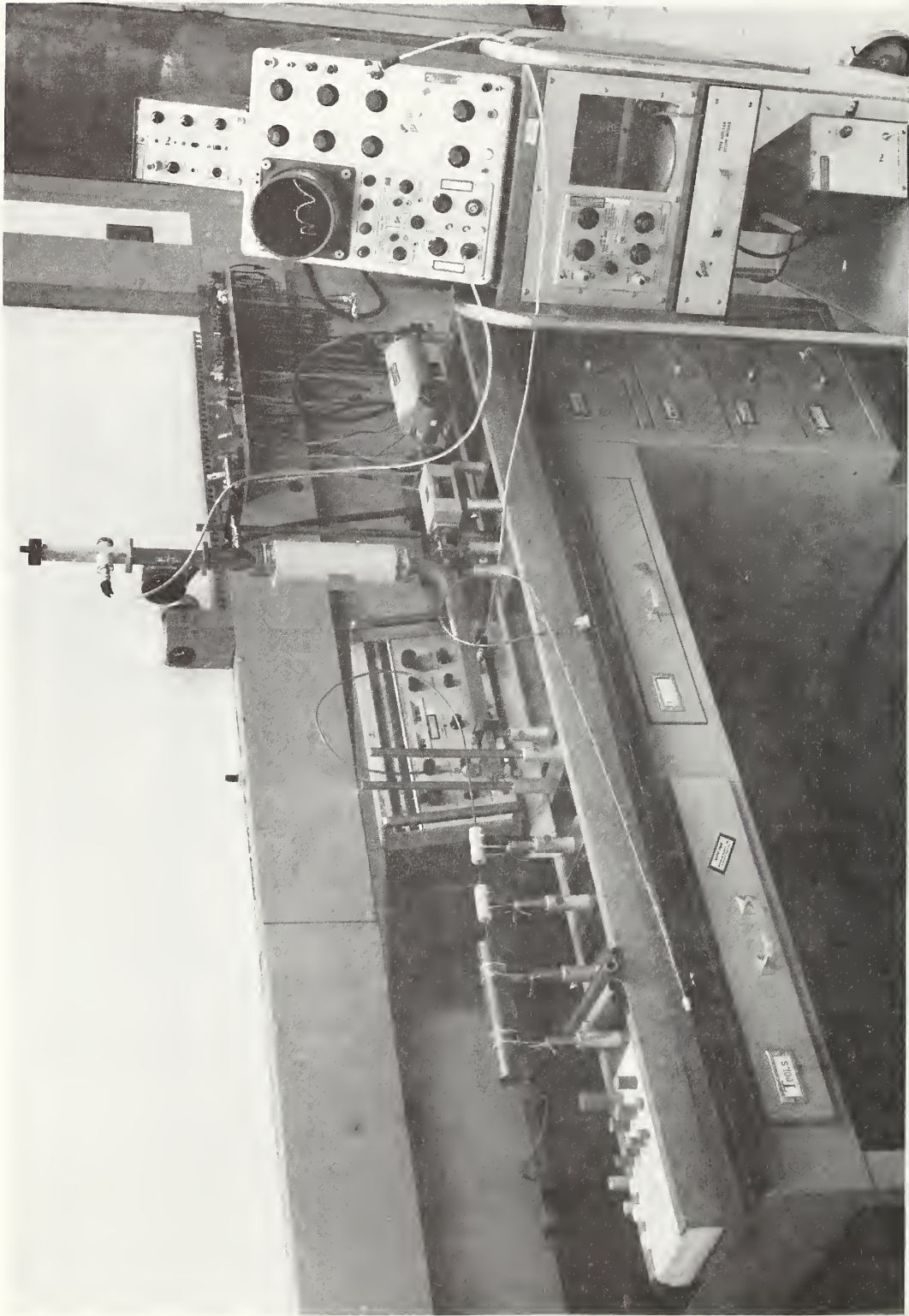


Figure 1. TE01 Circular Mode Dielectric Measurement System.

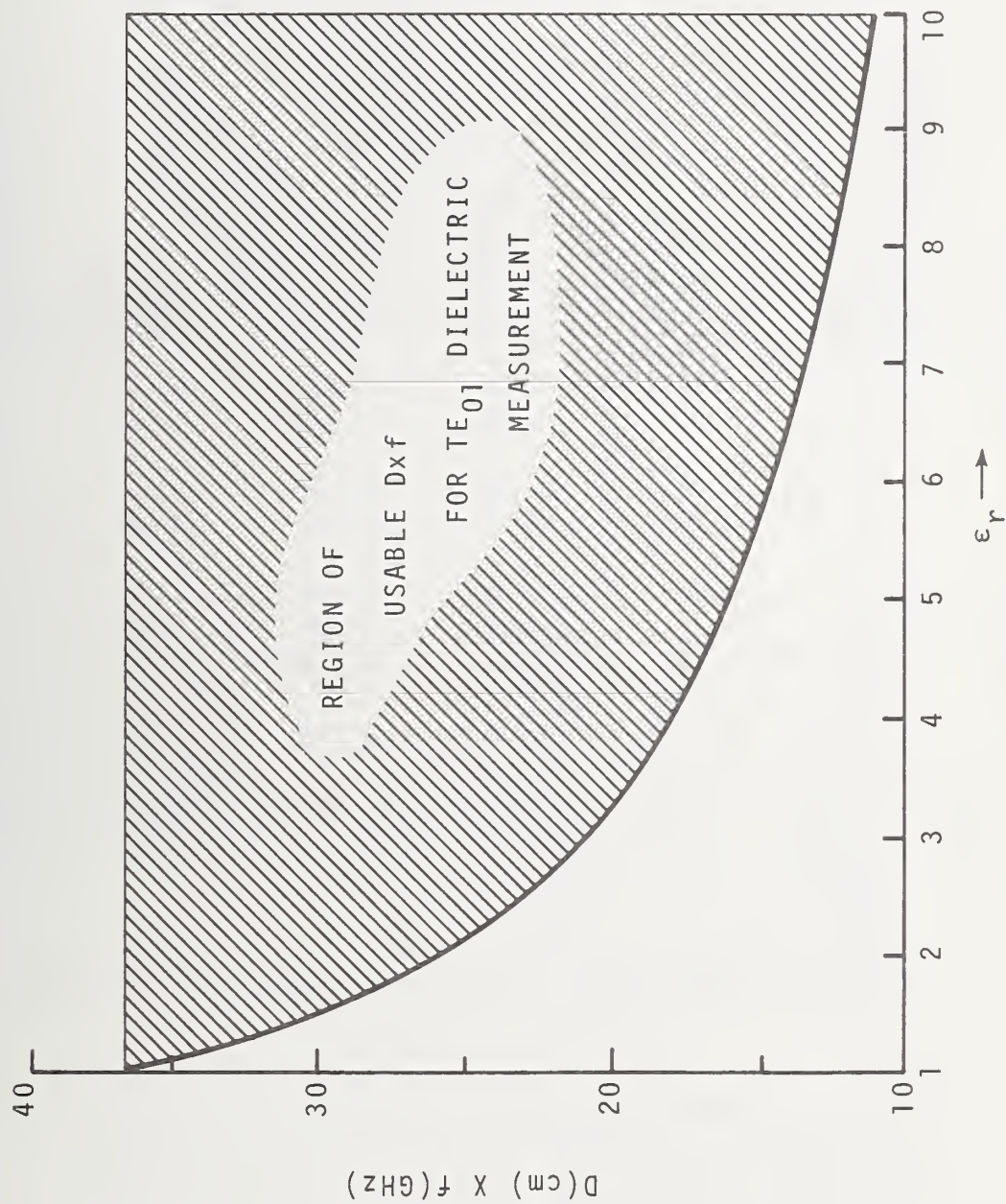


Figure 2. D-F Graph for TE₀₁ Measurement.

Tube	Tube Diameter (cm)	Sample Batch Number	Sample Diameter (cm)	Sample Length (cm)	Measured Frequency (GHz)	Relative Dielectric Constant	Loss Tangent
Cu	2.007	1	2.007	0.828	9.827	4.635	0.0009
Cu	2.007	1	2.007	0.808	9.917	4.632	0.0009
Cu	2.007	1	2.007	0.726	10.110	4.630	
Cu	2.007	1	1.999	0.726	10.115	4.625	
Cu	2.007	2	2.007	0.772	10.016	4.634	
Coax	14 mm	2		5 cm	8.486	4.489	
Coax	14 mm	2		5 cm	10.000	4.492	
Al	1.895	1	*	0.726	10.589	4.636	0.0013

*Diameter reduced by hand to fit tube. Bad job - visible air gap between sample and tube.

Figure 3. Table of TE01 Measurements for Various Materials.

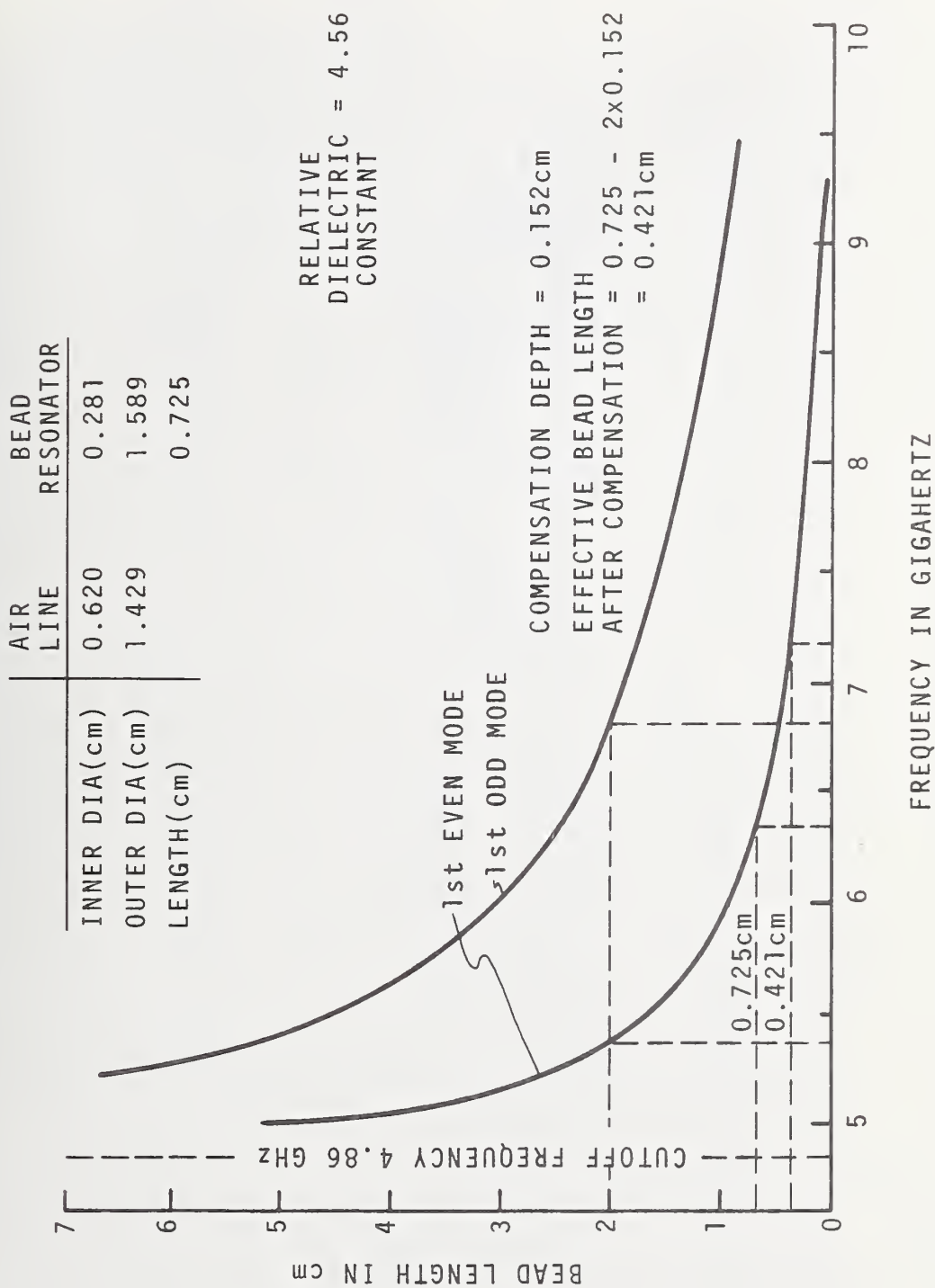


Figure 4. Bead Resonant Frequencies for TELL Circular Mode in 14 mm Bead.

	AIR LINE	BEAD RESONATOR	BEAD
INNER DIA.(cm)	0.620	0.281	0.281
OUTER DIA.(cm)	1.429	1.589	1.589
LENGTH (cm)		0.725	0.725

$$\epsilon_r = 4.56$$

$$f_0 = 19.35\text{GHz} \sim 360^\circ$$

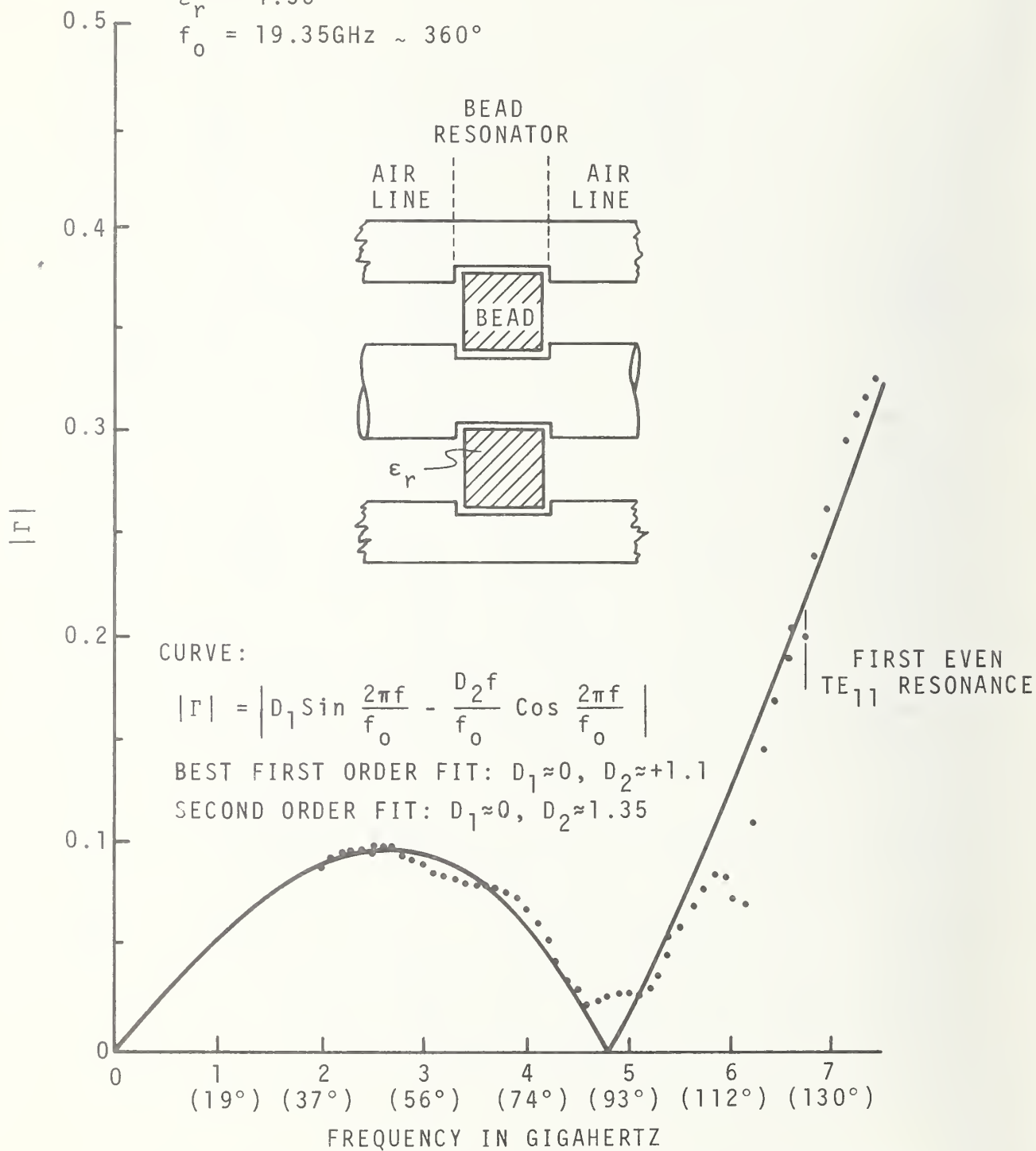


Figure 5. Measurement Data for 14 mm Bead-Line Before Compensation.

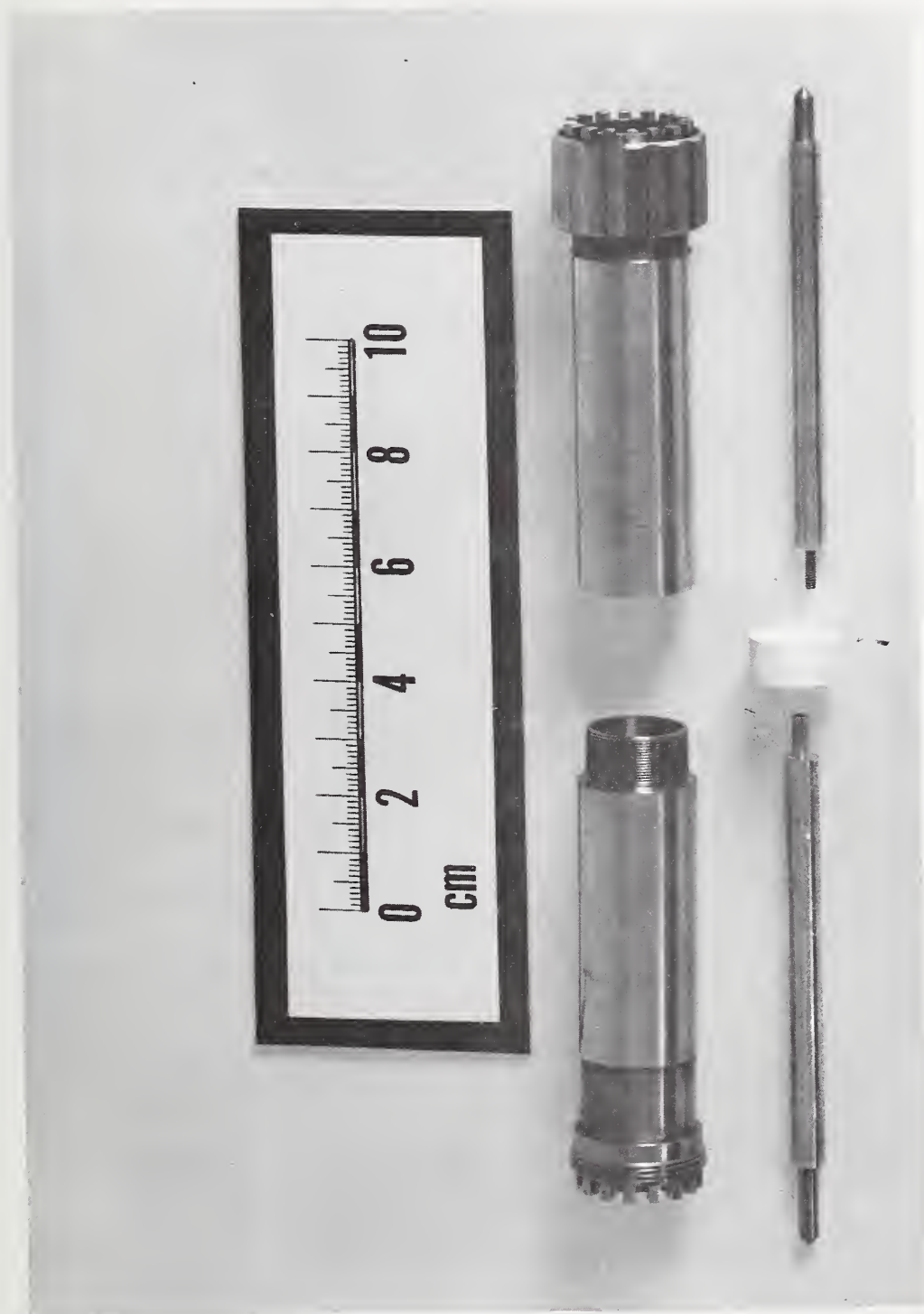


Figure 6. 14 mm Bead and Line.

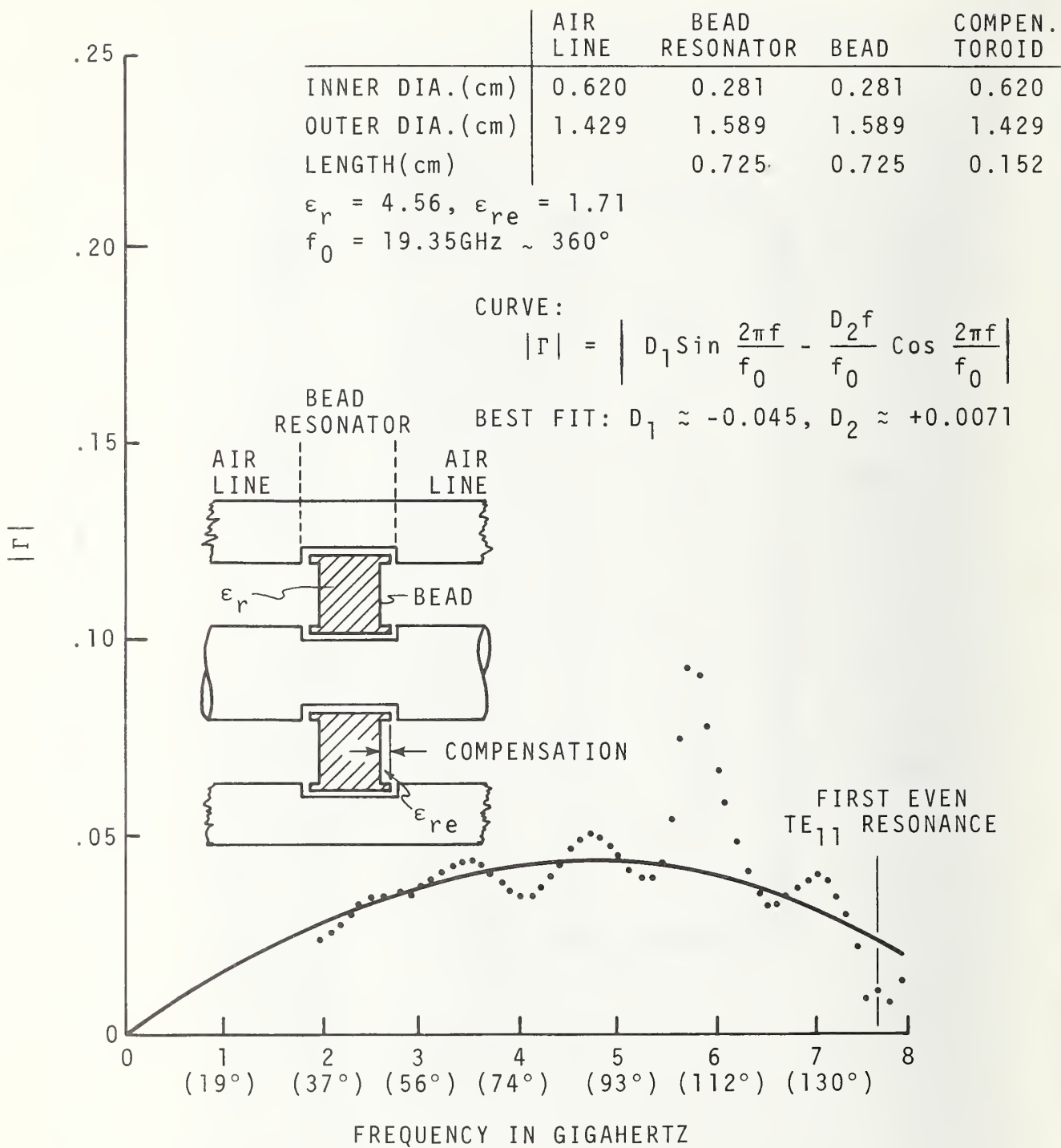


Figure 7. Measurement Data for 14 mm Bead-Line After Compensation.

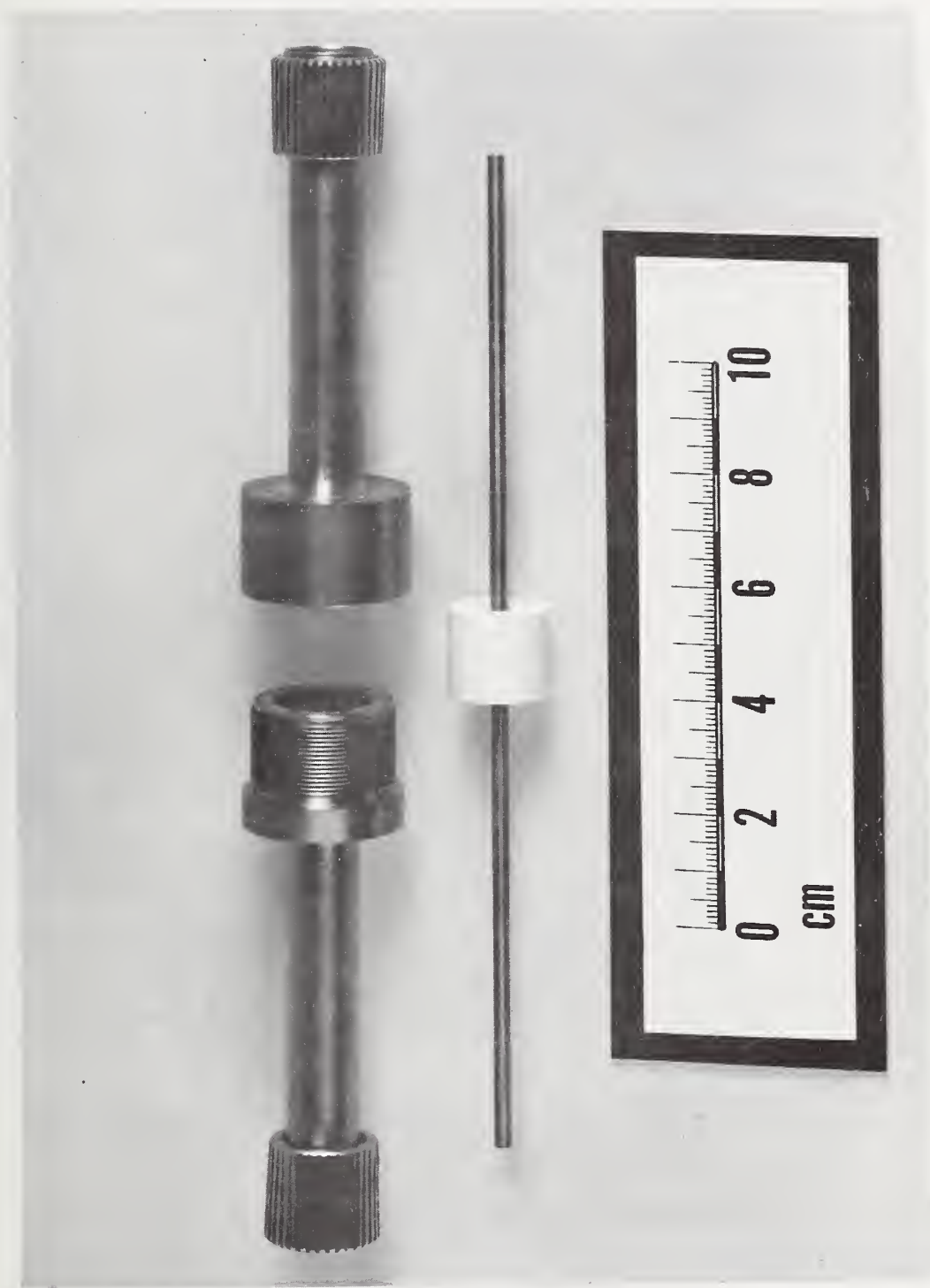


Figure 8. 7 mm Bead and Line.

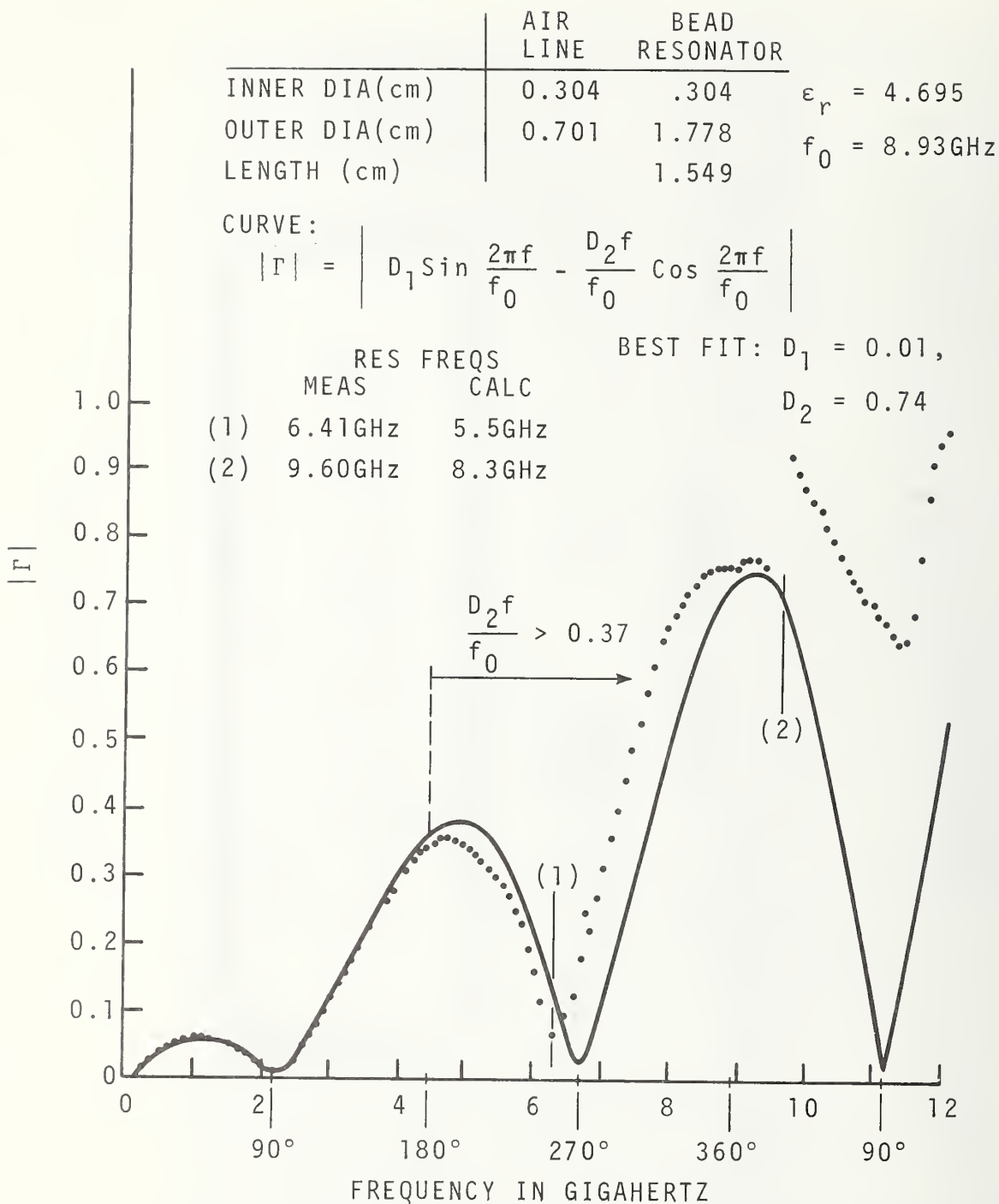


Figure 9. Measurement Data for 7 mm Bead-Line Before Compensation.

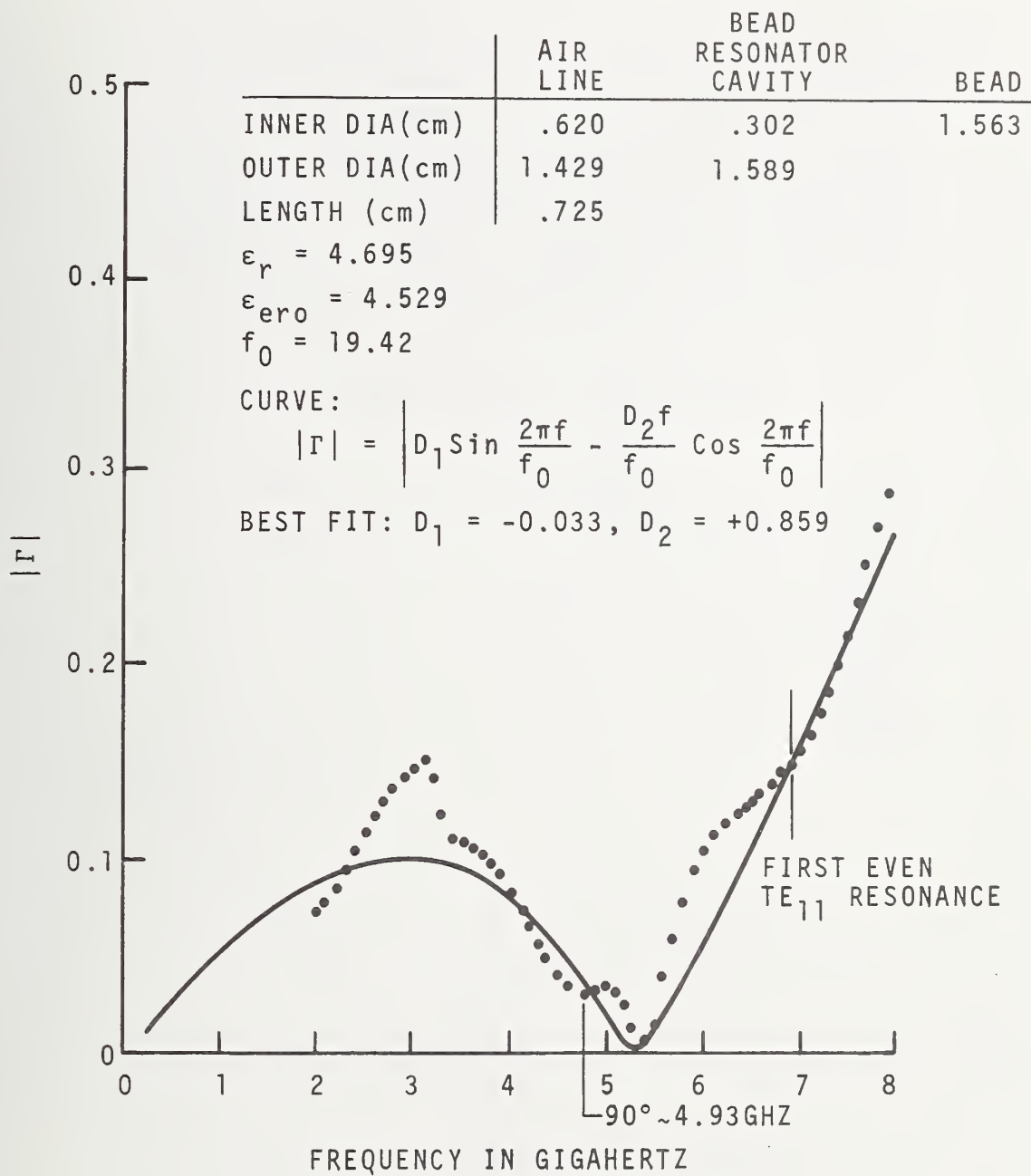


Figure 10. Measurement Data for 14 mm Bead-Line-Gap Before Compensation.

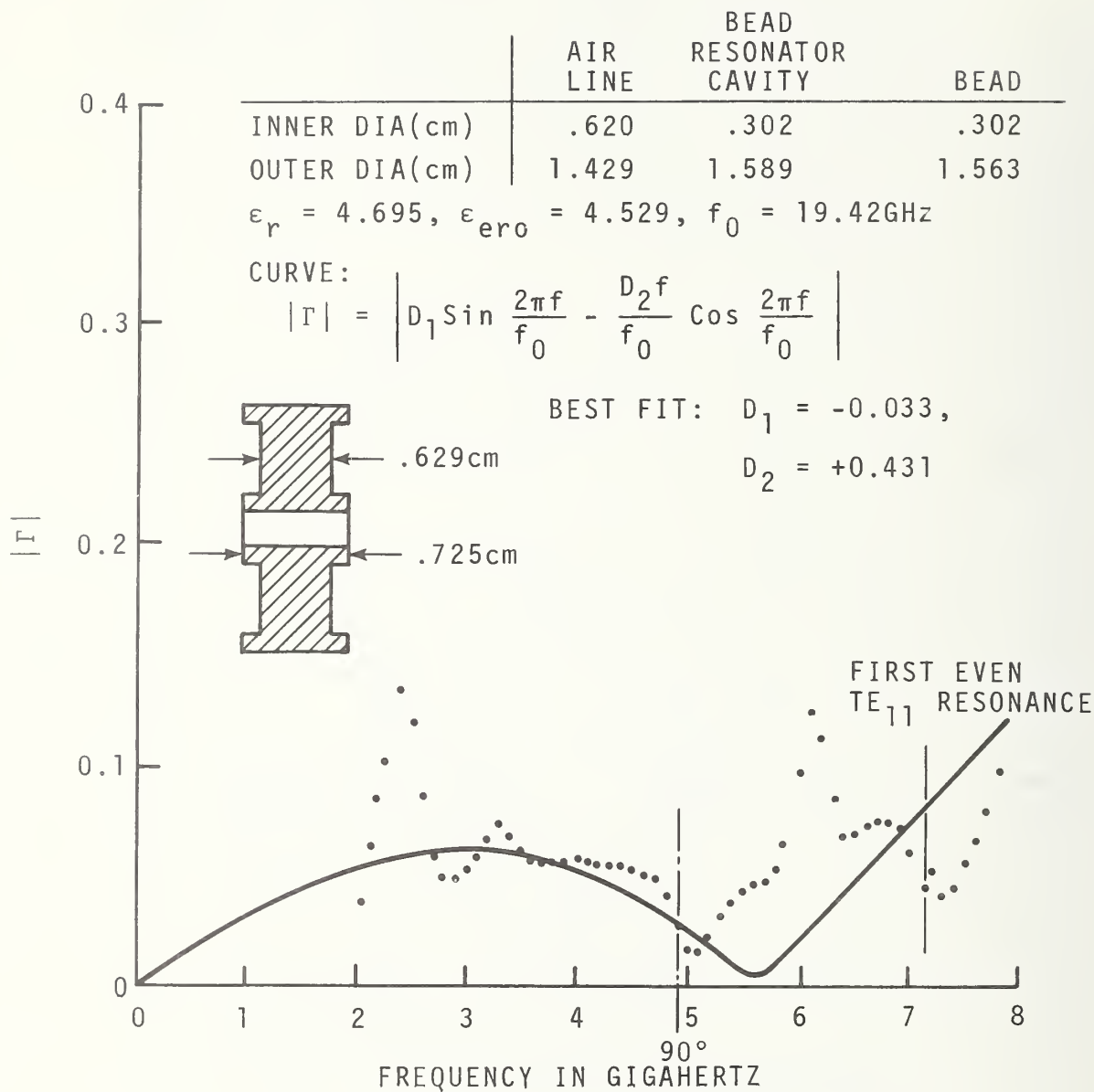


Figure 11. Measurement Data for 14 mm Bead-Line-Gap After Compensation.

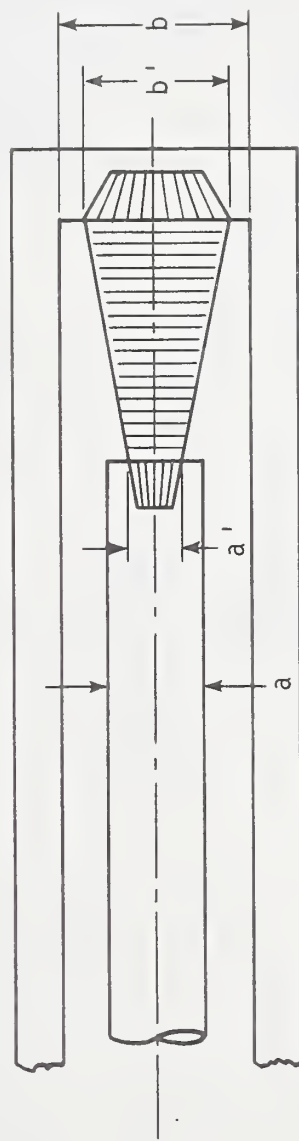
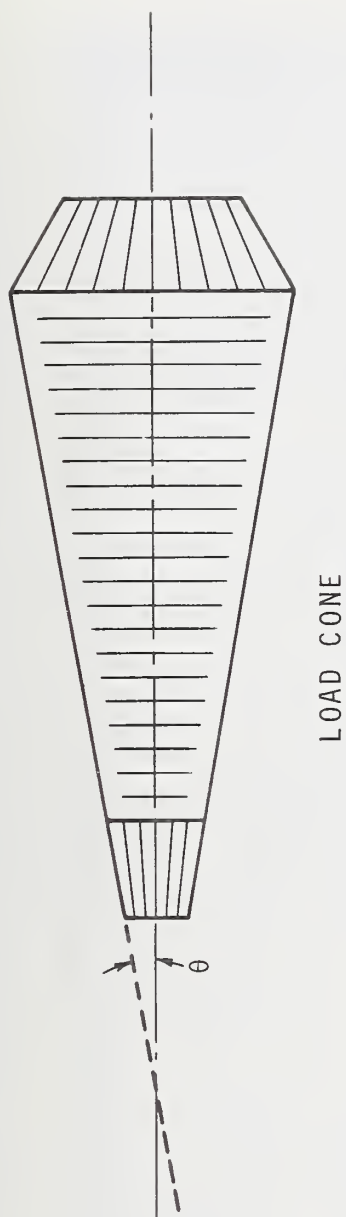


Figure 12. Resistive Cone and Cone Holder for 7 mm Termination.

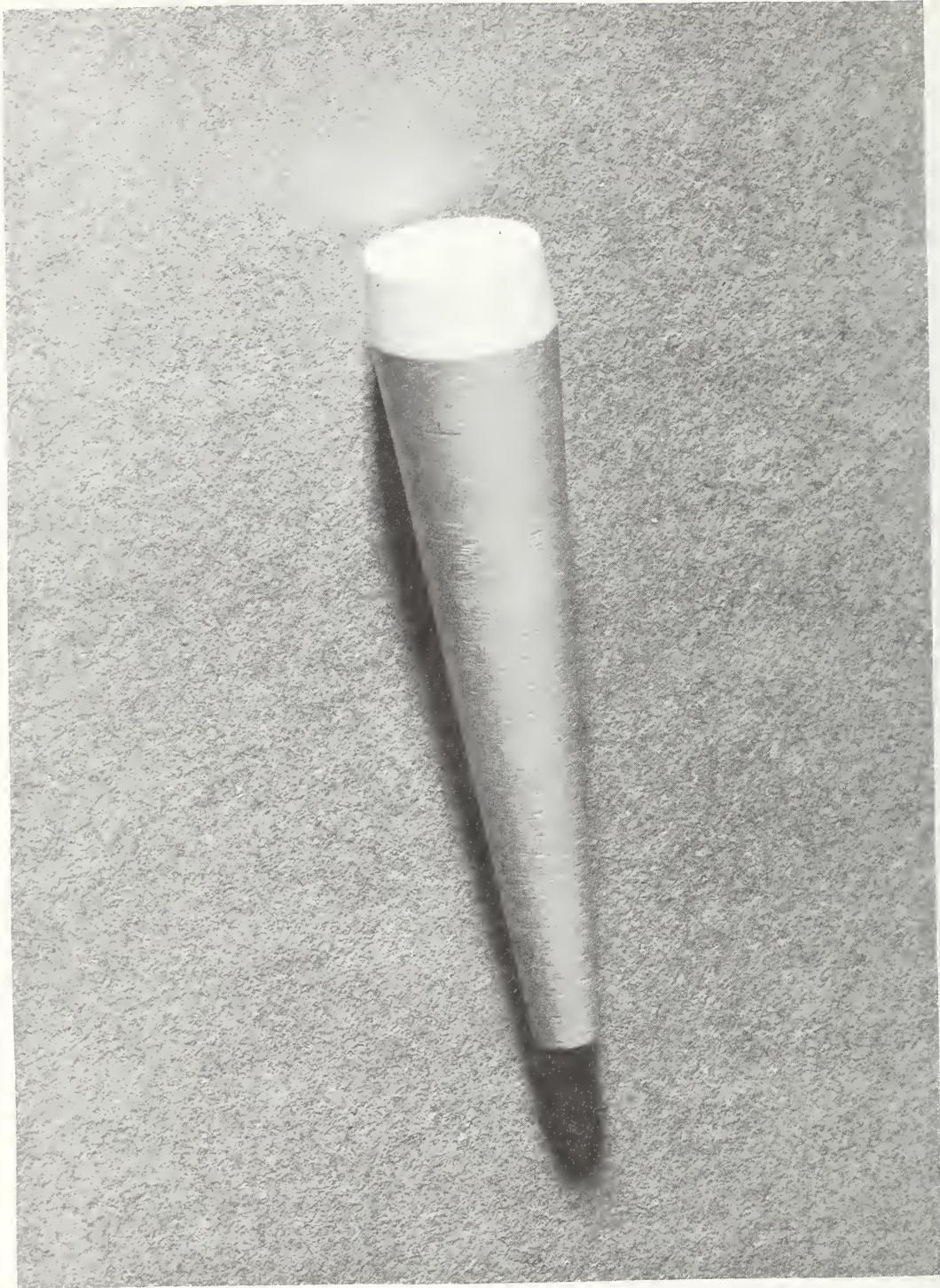


Figure 13. Resistive Cone.

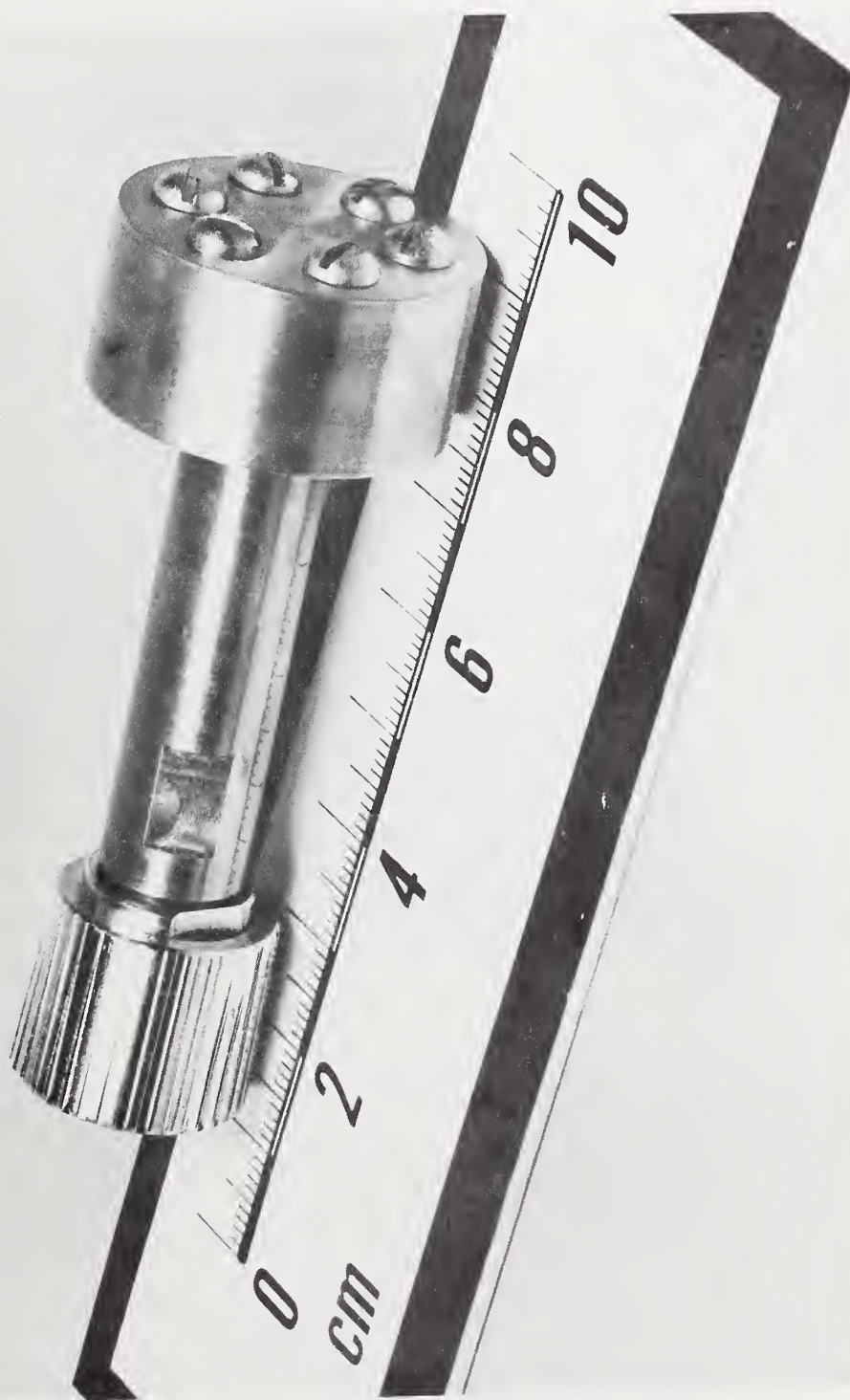


Figure 14. Cone Holder.

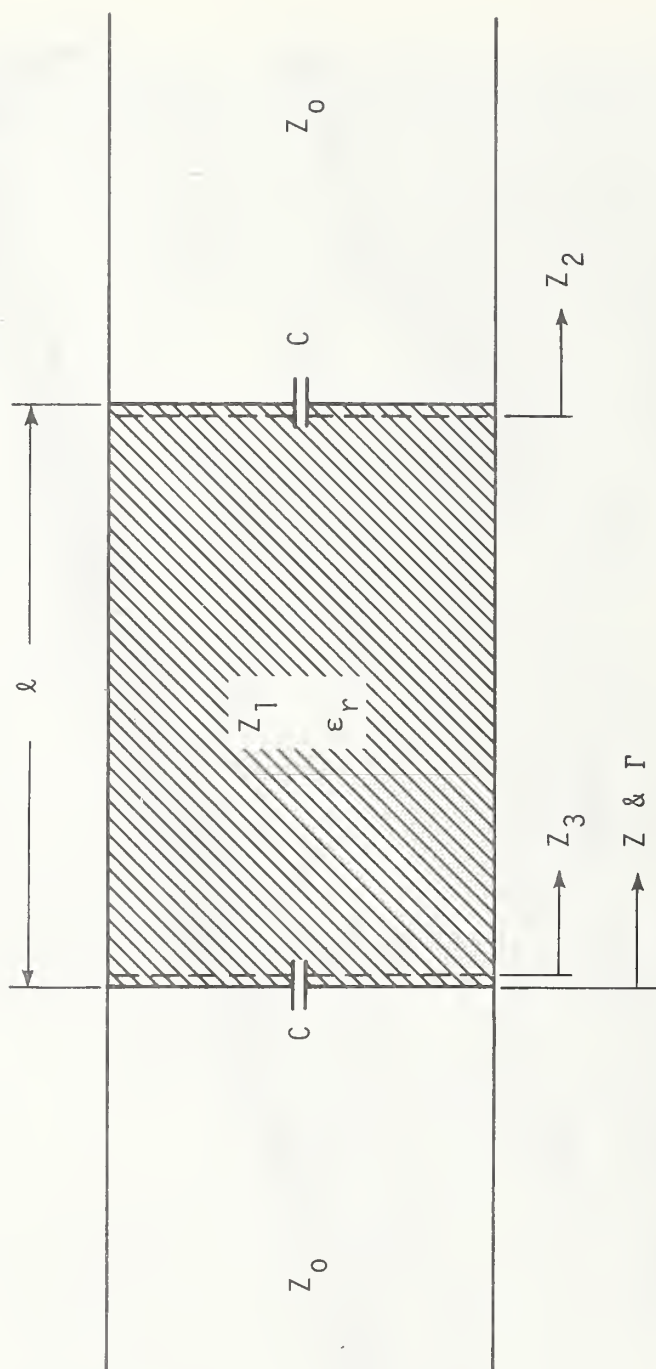


Figure 15. Equivalent Circuit for Derivation of Equation G.11.

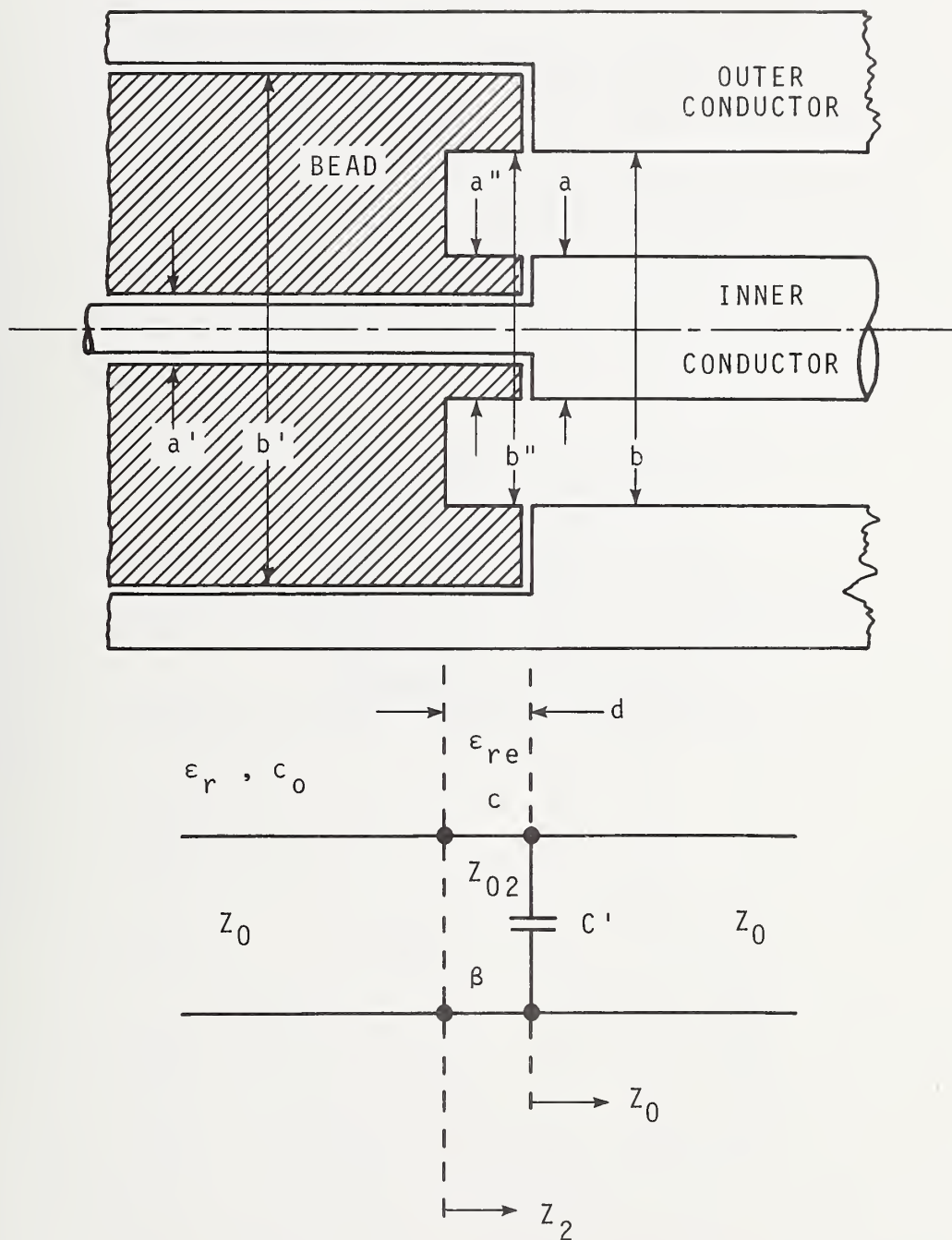


Figure 16. Profile View and Equivalent Circuit for Derivation of Equation I.11.

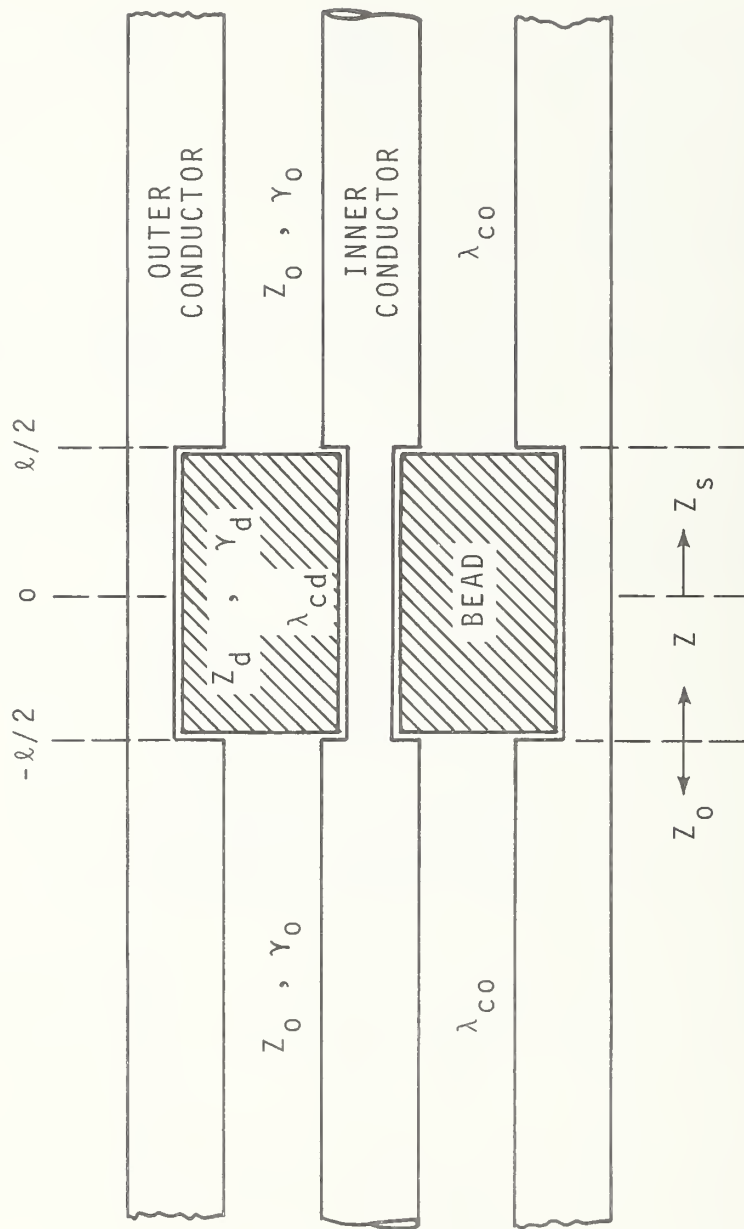


Figure 17. Profile View for Derivation of Equation J.6.

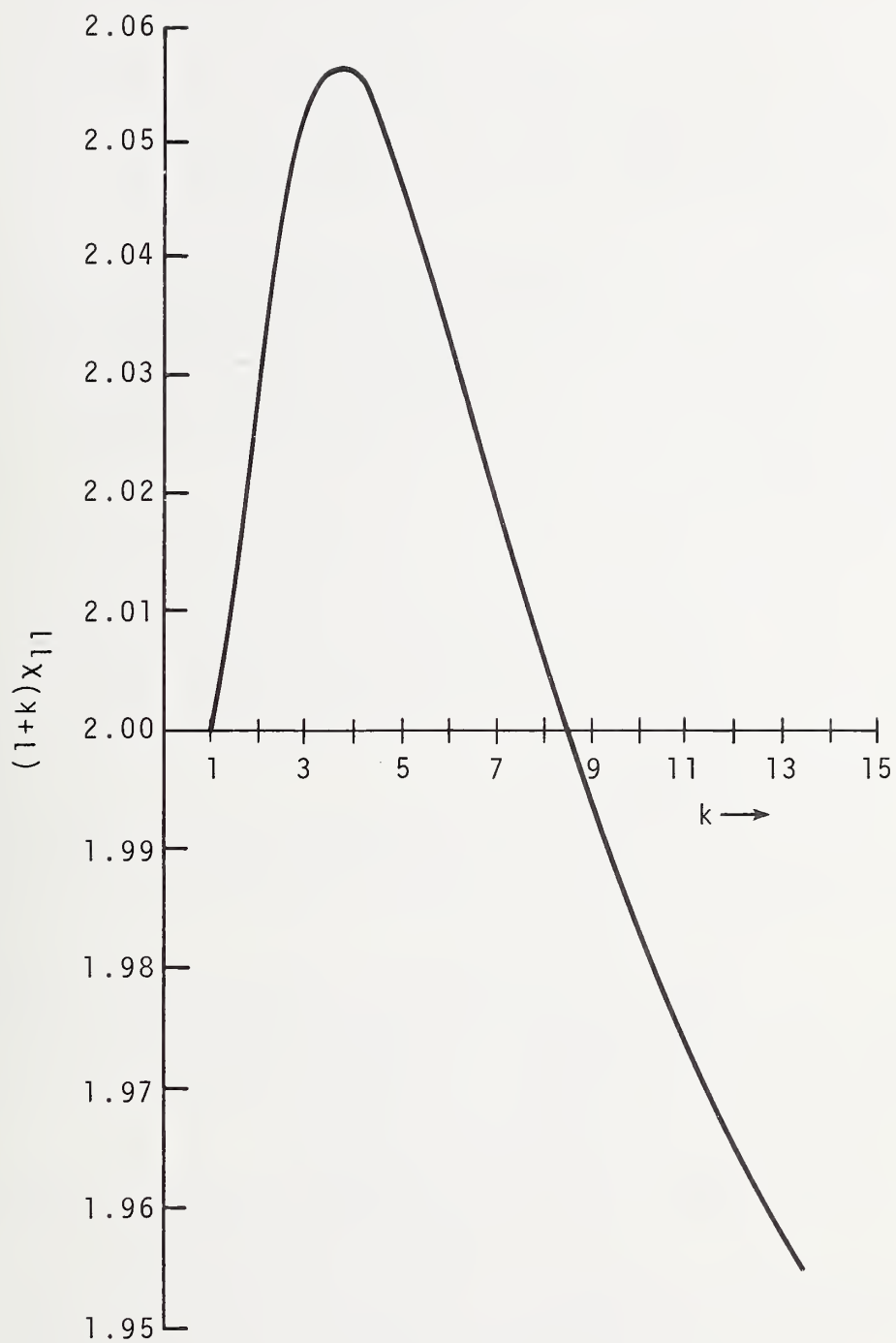


Figure 18. Graph of $(1 + k)X'_{11}$.

APPENDIX A

CCG Work Statement

A. Project Title: Reference Noise Standard Development

B. Objective:

1. General: To develop an excess noise reference standard to provide a basis for support of waveguide and coaxial noise sources in use within the Department of Defense.

2. FY 1973 Work Statement:

a. Investigate and establish the direction for the design and development of a calculable reference standard noise source meeting the following technical requirements:

- (1) Output Level: Optimize for use with the AIL type 82 system.
- (2) Frequency Range: At least 100 MHz to 12 GHz.
- (3) Stability: Suitable for use as a primary reference standard for eight years.
- (4) Output Connector Type: Selected to minimize comparison errors when calibrating standards with waveguide, 14 mm, 7 mm, 3.5 mm and type N precision connectors.
- (5) Operation Requirements: Suitable for operation by standards laboratory personnel.

(6) Physical Requirements: Suitable for operation in a standards laboratory and capable of being transported between laboratories.

b. Prepare a detailed report on the noise source requirements and investigation results.

C. Background: The requirement exists within DOD to measure the operating noise figure of RADAR, missile, ECM and communications receivers using automatic noise figure meters and excess noise sources. The reliability of these measurements depend, among other things, upon the accuracy in the excess noise ratio value (dB) assigned to the noise source by DOD calibration laboratories. Over the frequency range of 0.5 to 7 GHz, these values are not tested due to the lack of a primary reference within DOD and at NBS. The major thrust of this effort is to provide the basis to fill this gap in our measurement system.

D. Approach:

1. Investigate and establish the direction for the design and development of a calculable reference standard noise source. Prepare a report documenting the noise source requirements and the investigation results.
2. Develop and evaluate design approaches for a reference standard noise source. Prepare a report documenting the design approaches, test results and the proposed design for a prototype standard.

3. Develop and evaluate a prototype reference standard noise source meeting stated technical specifications. Prepare a report including a description of the development and evaluation of the prototype, design drawings and test and operating instructions.

E. Milestones:

1. Evaluate loss, VSWR and repeatability on required coaxial connectors to determine the effects on final accuracies and decide on transmission line dimensions. 3 Aug 72
2. Estimate feasible temperature distribution for transmission lines necessary to achieve reasonable accuracy. 30 Sep 72
3. Complete accurate determination of dielectric constants for proposed bead materials. 31 Oct 72
4. Establish feasible design of a broadband, low VSWR transmission line using beads to support the inner conductor. 31 Dec 72
5. Determine feasibility of using heat pipes to achieve required temperature distribution of transmission line. 31 Jan 73
6. Complete investigation of tractrix design at room temperature for a broadband low VSWR termination. 28 Feb 73

7. Complete evaluation of feasibility of the manner 30 Apr 73
of bead supporting the inner-conductor for 1000°C
application.
8. Complete the determination of the design for the 30 Jun 73
termination required to achieve a broadband low
VSWR termination that will withstand temperature
cycling to 1000°C. Complete final report for this
phase of the project.

APPENDIX B

Output Noise Temperature for a Coaxial Thermal Noise Source

First Order Calculation

An approximate expression for the noise temperature of a coaxial thermal noise source is developed in this appendix. This equation takes into account the different temperature and resistivity distributions along the inner and outer conductors respectively.

The development starts from equation (N.2) of NBS Technical Note 615⁽¹⁾ which gives the output noise temperature, T , of a thermal noise source in kelvins.

$$T = T_m \alpha_o + \int_0^l T_x \alpha'_x dx \quad (\text{B.1})$$

where T_m is the physical temperature (in kelvins) of the resistive element terminating the line; α_o is the available power ratio (less than unity) of the line from the termination at $x=0$ to the output connector at $x=l$, T_x is the physical temperature (in kelvins) at x of the inner and outer conductor of the line; and α'_x is the gradient at x of the available power ratio of the line. The first term in equation (B.1) is the noise from the generating resistor attenuated by the line arriving at the output connector from the termination, while the second term is the noise generated by the line arriving at the output connector. The line is assumed to be slightly lossy, but otherwise ideal. The connector is assumed to be lossless and reflectionless.

The second term can be rewritten as

$$\int_0^l \left(\frac{T_x \alpha'_x dx}{\alpha_x} \right) \alpha'_x \quad (\text{B.2})$$

where the parenthetical factor is the noise power generated in the elemental piece of line dx at x . This factor applies to the case where the inner and outer conductor have the same temperature and resistivity distributions as a function of x along their lengths. The purpose of this appendix is to develop an approximation for this factor that applies to a coaxial line where both distributions may be different.

The factor α'_x / α_x will not in general separate into a sum of two terms, one representing the inner conductor loss and one representing the outer conductor loss. Therefore, it is not possible in general to determine how much of the noise is generated in either conductor separately, a determination made important by the differing temperature distributions of the inner and outer conductors. However, to first order in the propagation constant (Appendix C) this factor is separable, allowing a separation of the noise into a contribution from the inner and from the outer conductors.

From Technical Note 615

$$\alpha_x = \left(\frac{1 - \frac{\gamma_x^2}{\gamma_2^2}}{1 - \frac{\gamma_1^2}{\gamma_2^2}} \right) e^{-2 \int_x^l \alpha_y dy} \quad (\text{B.3})$$

where

$$|\Gamma_x| = |\Gamma_g| e^{-2 \int_0^x \alpha_y dy}$$

$$|\Gamma_x| \equiv |\Gamma_{x=l}|$$

and where α_y is the real part of the propagation constant for the principle or TEM mode. Γ_g is the reflection coefficient of the terminating element.

From (B.3) it can be shown that

$$\frac{\alpha'_x}{\alpha'_{-x}} = 2 \alpha_x \left(\frac{1 + |\Gamma_x|^2}{1 - |\Gamma_x|^2} \right) \quad (\text{B.4})$$

Since Γ_x is the reflection coefficient looking toward the termination from the elemental segment of line dx at x and does not involve dx itself, only α_x characterizes the loss of dx and consequently the noise generated by it. α_x does not separate into a simple linear combination representing the inner and outer conductor losses. However, to first order α_x becomes (Appendix C)

$$\alpha_x = \alpha_{xi} + \alpha_{xo} \quad (\text{B.5})$$

in which case

$$\frac{\alpha'_x}{\alpha_x} = 2(U_{xi} + U_{xo}) \left(\frac{1 + |T_x|^2}{1 - |T_x|^2} \right) \quad (\text{B.6})$$

Since the inner and outer conductor losses are now separate and identifiable their separate noise contributions can also be identified.

Correspondingly, if the inner and outer conductors have temperature distributions T_{xi} and T_{xo} respectively, the noise from dx is given by

$$2(T_{xi}U_{xi} + T_{xo}U_{xo}) \left(\frac{1 + |T_x|^2}{1 - |T_x|^2} \right) dx \quad (\text{B.7})$$

This noise is attenuated by α_x before it reaches the end of the line at the output connector. Thus the total noise output from the line is

$$2 \int_0^l (T_{xi}U_{xi} + T_{xo}U_{xo}) \left(\frac{1 + |T_x|^2}{1 - |T_x|^2} \right) \alpha_x dx \quad (\text{B.8})$$

which is the sum of the attenuated noise contributions from each of the elemental line segments.

When the attenuated noise power $T_m \alpha_o$ from the termination is added to (B.8), the noise output T from the source is

$$T = T_m \alpha_o + 2 \int_0^l (T_{xi}U_{xi} + T_{xo}U_{xo}) \left(\frac{1 + |T_x|^2}{1 - |T_x|^2} \right) \alpha_x dx. \quad (\text{B.9})$$

Error in the First Order Calculation

By assuming a single average temperature distribution for the inner and outer conductors which is flat from the termination to some point where the distribution goes through a transition to room temperature and is again flat out to the output connector, an order of magnitude estimate of the relative error δT in the noise temperature T is obtained and is given by

$$\frac{\delta T}{T} \approx \frac{\Delta T_1}{T_m} \cdot \frac{\Delta T_2}{\Delta T_1} \quad (\text{B.10})$$

The first factor $\Delta T_1 / T_m$ is the relative correction to the termination temperature, and the second factor $\Delta T_2 / \Delta T_1$ is the relative error in this correction. Using the above distribution an estimate for the factors results in the following two equations:

$$\frac{\Delta T_1}{T_m} \approx \frac{1}{2^{1/2}} \frac{R\ell}{Z_0} \left(\frac{T_0 - T_m}{T_m} \right) \quad (\text{B.11})$$

and

$$\frac{\Delta T_2}{\Delta T_1} \approx \frac{R}{\omega L_0} \quad (\text{B.12})$$

ℓ is the length of line from the start of the temperature transition to the output of the source, R is the average resistance per unit length for the length of line ℓ , T_0 is room temperature, Z_0 is the characteristic line impedance, and L_0 is the line inductance per unit length.

For the standard envisioned in this report the relative error calculated from equation (B.10) is of the order of 10^{-7} .

APPENDIX C

Propagation Constant of a Coaxial Line

The real part α of the propagation constant for the TEM mode in a coaxial line is given by ⁽¹⁰⁾

$$\alpha = Z^{-1/2} \left\{ [(R^2 + \omega^2 L^2)(G^2 + \omega^2 C^2)]^{1/2} + RG - \omega^2 LC \right\}^{1/2} \quad (C.1)$$

where

$$R = \left(\frac{f}{\pi} \right)^{1/2} \left[\frac{(\rho_i \mu_i)^{1/2}}{D_i} + \frac{(\rho_o \mu_o)^{1/2}}{D_o} \right] \equiv R_i + R_o$$

$$L = L_o + \frac{R}{\omega}, \quad L_o = \frac{\mu_o}{2\pi} \ln D_o/D_i$$

and

$$C = \frac{2\pi \epsilon_o \epsilon_r}{\ln D_o/D_i}$$

D_i = outer diameter of inner conductor,

D_o = inner diameter of outer conductor,

f = frequency in hertz

ω = $2\pi f$

ρ_i = resistivity of inner conductor in ohm-meters,

ρ_o = resistivity of outer conductor in ohm-meters,

μ_a = magnetic permeability of the dielectric (air) between conductors in henry/meter,

μ_i = magnetic permeability of inner conductor in henry/meter,

μ_o = magnetic permeability of outer conductor in henry/meter,

ϵ_o = dielectric constant of free space in farad/meter,

ϵ_r = relative dielectric constant of dielectric (air),

R = resistance in ohms/meter,

L = inductance in henrys/meter,

C = capacitance in farads/meter,

G = conductance in mhos/meter (zero for air dielectric).

To second order in $R/\omega L_o$ and $G/\omega C$

$$u = \frac{\omega(L_o C)^{1/2}}{2} \left(\frac{R}{\omega L_o} + \frac{G}{\omega C} + \frac{RG}{2\omega^2 L_o C} - \frac{R^2}{2\omega^2 L_o^2} \right) \quad (C.2)$$

For a line containing a perfect dielectric ($G = 0$), to second order in $R/\omega L_o$

$$u = \frac{\omega(L_o C)^{1/2}}{2} \frac{R}{\omega L_o} \left(1 - \frac{R}{2\omega L_o} \right) \quad (C.3)$$

which reduces to first order in $R/\omega L_o$ when

$$R \ll \omega L_o. \quad (C.4)$$

When (C.4) holds, u can be written as

$$u = u_i + u_o \quad (C.5)$$

where

$$u_i = \frac{\omega(L_0 C)^{1/2}}{2} \frac{R_i}{\omega L_0} \quad (C.6)$$

and

$$u_0 = \frac{\omega(L_0 C)^{1/2}}{2} \frac{R_0}{\omega L_0} . \quad (C.7)$$

APPENDIX D

Design Formula for the TE₀₁ Circular Mode Resonance Measurement

An intuitive picture of the relative dielectric constant measurement⁽²⁾ using the TE₀₁ circular resonance in a waveguide-below-cutoff cylinder containing a sample of the material under consideration can be drawn as follows. Consider a hollow air-filled cylinder which is below cutoff for a particular waveguide mode, but which is above cutoff inside a dielectric material sample located in the cylinder. Then for a particular length of such a sample there exists a particular frequency for which the cylinder and sample act as a resonant cavity at its resonance frequency. This frequency is uniquely related to the sample length, the diameter of the cylinder, and the dielectric constant of the sample. Therefore, if the length and diameter are known, the measurement of the resonant frequency will yield the dielectric constant of the sample. It will clearly work only when the mode propagation constant is real inside the sample and imaginary outside. From Appendix E it can be seen that this requirement implies that

$$\lambda_c^2 < \lambda^2 < \lambda_c^2 \epsilon_r$$

where λ is the free space wavelength, λ_c is the cutoff wavelength in the sample free part of the cylinder, and ϵ_r is the relative dielectric constant of the sample material. In terms of the frequencies corresponding to these wavelengths,

$$f_c > f > f_c \epsilon_r^{-1/2} \quad (\text{D.1})$$

defines the range of frequencies over which a resonance can be expected to work (figure 2).

The circular TE01 mode is particularly useful in high temperature measurements since its electric field vanishes at the cylinder walls. Therefore, the resulting measurement of ϵ_r is much less susceptible to error from air gaps between the sample and the cylinder, allowing the cylinder and sample to be heated without introducing large errors. A useful expression for ϵ_r is (Appendix E with $A = 1$)

$$\epsilon_r = \frac{\lambda^2}{\lambda_{gd}^2} + \frac{\lambda^2}{\lambda_c^2} \quad (\text{D.2})$$

where λ_{gd} is the guide wavelength in the dielectric.

For the TE01 mode in a sample of length L to resonate λ_{gd} is given by⁽²⁾

$$\lambda_{gd} = \frac{\pi L}{y} \quad (\text{D.3})$$

where y is a solution of the equation

$$y \tan y = C$$

and

$$C \equiv \frac{\pi L}{\lambda} \left(\frac{\lambda^2}{\lambda_c^2} - 1 \right)^{1/2}$$

The cutoff wavelength for a particular diameter D is given by⁽¹¹⁾

$$\lambda_c = 0.820D \quad (D.4)$$

for this mode.

APPENDIX E

Propagation Constant in a Lossy Dielectric

This appendix contains an expression for the propagation constant that is used in the two preceding appendices and is given here for convenient reference.

The propagation constant for a particular mode in an ideal waveguide of cylindrical symmetry filled with a lossy dielectric is given by ⁽¹¹⁾

$$\gamma = \alpha + j\beta \quad (\text{E.1})$$

where

$$\alpha = \frac{\beta \tan \delta}{2 \epsilon_r^{1/2}}$$

$$\beta = \beta_0 \epsilon_r^{1/2} \epsilon_1$$

$$\beta_0 = \frac{2\pi}{\lambda}$$

$$\epsilon_1 = 2^{-1/2} \left(1 - \frac{\lambda^2}{\lambda_0^2 \epsilon_r} \right)^{1/2} \left[1 + \left(1 + \frac{\tan^2 \delta}{(1 - \lambda^2 / \lambda_0^2 \epsilon_r)^2} \right)^{1/2} \right]^{1/2}$$

$$\lambda_{gd} = \frac{2\pi}{\beta}$$

In these expressions $\tan \delta$ is the dielectric loss tangent, ϵ_r is the relative dielectric constant (Appendix F), λ is the free space wavelength, λ_{gd} is the

guide wavelength in the dielectric, and λ_c is the cutoff wavelength for the air filled guide. λ_c is infinite for the TEM mode of propagation.

These expressions can be manipulated to give the following expression for ϵ_r :

$$\epsilon_r = \frac{\lambda^2}{\lambda_c^2} + \frac{A^2 \lambda^2}{\lambda_{gd}^2} \quad (E.2)$$

where

$$A \equiv \frac{1}{\xi_1} \left(1 - \frac{\lambda^2}{\lambda_c^2 \epsilon_r} \right)^{1/2} .$$

For most cases ϵ_r is given by equation (E.2) with A equal to one. For large loss tangents however a better value for ϵ_r is given by equation (E.2) by iteration, starting with A equal to one, obtaining the first approximation to ϵ_r , and proceeding to iterate using the resulting value of A.

APPENDIX F

Dielectric Constant Measurement Using the Automatic Network Analyzer

The complex relative dielectric constant of a dielectric material completely filling a length of ideal waveguide is given by^(12, 13)

$$\epsilon = \epsilon' - j\epsilon'' = \epsilon_r (1 - j \tan \delta)$$

and is obtained from the ANA data as:

$$\begin{aligned} \epsilon &= \frac{\left(\frac{1 + S_{11}S_{22} - S_{12}S_{21}}{S_{11} + S_{22}} - 1 \right)}{\left(\frac{1 + S_{11}S_{22} - S_{12}S_{21}}{S_{11} + S_{22}} + 1 \right)} \\ &= \frac{(1 - S_{11})^2 - S_{12}^2}{(1 + S_{11})^2 - S_{12}^2} \end{aligned} \quad (\text{F.1})$$

where the S's represent the components of the 2 x 2 scattering matrix representing the length of dielectric filled waveguide section being measured. ϵ_r is the relative dielectric constant and is equal to ϵ' . $\tan \delta$ is the loss tangent and is the ratio of ϵ'' to ϵ' . The last expression obtains where the waveguide and material form a reciprocal junction.

These expressions are used in the following program written for the automatic network analyzer⁽¹³⁾:

ANA Program

```
5 DIM E[88],G[88]
6 PRINT
7 PRINT
10 REM DIELECTRIC ANALYSIS
15 LET Q1=Q2=Q3=Q4=Q9=0
20 DIM S[32],D[88,4],M[88],F[88],A[88],B[88]
25 LET C9=2.09650E-04
26 PRINT "AVERAGE DATA? ";
27 CALL (41,L1)
29 IF L1=0 THEN 26
30 CALL (3,S[11],0,1)
40 LET F=S[27]
50 FOR N=S[14] TO S[14]+INT((S[3]-1)/8)
60 LET N1=8*(N-S[14])+1
70 CALL (3,D[N1,1],0,N)
80 NEXT N
90 LET M1=1+(S[12]-S[11])/S[13]
100 FOR N=1 TO M1
110 LET F[N]=S[11]+S[13]*(N-1)
120 LET M[N]=1+(F[N]-S[11])/S[2]
130 NEXT N
150 REM CALC E PARAMETERS
155 CALL (14,1,0,C1)
156 IF L1=1 THEN 3000
160 FOR N=1 TO M1
170 LET K=M[N]
175 IF S[31]=-1 THEN 210
180 LET S1=D[K,1]
185 LET S2=D[K,2]
190 LET S3=D[K,2]
195 LET S4=D[K,1]
200 GOTO 230
210 LET S1=D[K,1]
215 LET S2=D[K,2]
220 LET S3=D[K,3]
225 LET S4=D[K,4]
230 CALL (12,S2,S3,C3)
235 CALL (12,S1,S4,C4)
240 CALL (10,S1,S4,C5)
245 CALL (10,C1,C4,C4)
250 CALL (11,C4,C3,C3)
255 CALL (13,C3,C5,C2)
260 CALL (11,C2,C1,C4)
265 CALL (10,C2,C1,C5)
270 CALL (13,C4,C5,C6)
280 CALL (15,C6,E[N],G[N])
290 LET G[N]=-G[N]
300 IF G[N]>0 THEN 315
```

```

310 LET G[N]=0
315 IF L1=1 THEN 400
320 NEXT N
330 PRINT
360 PRINT " FUNCTION ";
365 INPUT J
370 IF J=1 THEN 400
375 IF J=2 THEN 540
380 IF J=3 THEN 1000
385 IF J=4 THEN 9000
390 GOTO 360
400 REM
401 PRINT "TITLE?";
402 CALL (41,Q)
403 PRINT
410 PRINT "FREQ";TAB(13)"E'(MEAS)";TAB(27)"E''(MEAS)";
413 PRINT TAB(41)"N";TAB(53)"K"
420 PRINT
425 IF L1=1 THEN 445
440 FOR N=1 TO M1
445 IF E[N]<1 THEN 506
450 GOSUB 645
490 PRINT F[N];TAB(10);E[N];TAB(25);G[N];TAB(40);D2;TAB(55);D1
500 GOTO 508
506 PRINT "BAD DATA"
508 IF L1=1 THEN 610
510 NEXT N
520 PRINT
530 GOTO 360
540 PRINT
550 PRINT "TITLE ?";
560 CALL (41,Q)
610 PRINT
611 PRINT "          LOSS          REFL LOSS";
615 PRINT " RESISTIVITY WAVELENGTH"
620 PRINT "FREQ";TAB(14)"(DB/IN)";TAB(28)"(DB-1AX)";
625 PRINT TAB(41)"(OHM-CM)";TAB(58)"(IN)"
630 PRINT
635 IF L1=1 THEN 641
640 FOR N=1 TO M1
641 IF E[N]<1 THEN 740
643 GOSUB 645
644 GOTO 720
645 LET K4=SQR(E[N]2+G[N]2)
650 LET D1=SQR(.5*(K4-E[N]))
660 LET D2=SQR(.5*(K4+E[N]))
670 LET D3=3.686*09*D1*F[N]*2.54
680 LET D4=11802.3/(F[N]*D2)
690 LET D5=((1+D2)2+D12)/((1-D2)2+D12)
695 LET D5=D5/(D5-1)
700 LET D6=4.343*LOG(D5)
704 IF G[N]>0 THEN 710

```



```

706 LET D7=1.033000E+20
708 GOTO 715
710 LET D7=1.800000E+06/(G[N]*F[N])
715 RETURN
720 PRINT F[N];TAB(10);D3;TAB(25);D6;TAB(40);D7;TAB(55);D4
730 GOTO 745
740 PRINT "BAD DATA"
745 IF L1=1 THEN 9000
750 NEXT N
760 GOTO 330
1000 REM PLOT ROUTINE
1020 PRINT "SET PAPER SCALE ?";
1030 CALL (41,0)
1040 IF Q=1 THEN 1130
1050 IF Q=-1 THEN 1200
1060 GOTO 1010
1130 CALL (40,15,J1)
1135 WAIT (500)
1140 IF J1<0 THEN 1195
1150 CALL (40,0,J2)
1160 IF J2<0 THEN 1170
1165 GOTO 1185
1170 CALL (43,255,255,1)
1180 GOTO 1130
1185 CALL (43,0,0,1)
1190 GOTO 1130
1195 CALL (43,0,0,1)
1200 REM
1260 CALL (43,255,0,1)
1262 LET J8=2
1265 PRINT "PLOT TYPE,SCALE ";
1270 INPUT J9,J8
1275 IF J9=10 THEN 360
1280 IF J9<1 THEN 1265
1290 IF J9>10 THEN 1265
1300 FOR N=1 TO M1
1310 IF J9=1 THEN 1400
1320 IF J9=2 THEN 1420
1330 IF J9=7 THEN 1440
1335 GOSUB 645
1340 IF J9=3 THEN 1500
1350 IF J9=4 THEN 1520
1360 IF J9=5 THEN 1540
1370 IF J9=6 THEN 1560
1380 IF J9=8 THEN 1580
1390 IF J9=9 THEN 1600
1400 LET Y=E[N]
1410 GOTO 1700
1420 LET Y=G[N]
1430 GOTO 1700
1440 LET Y=E[N]/G[N]
1450 GOTO 1700

```

```

1500 LET Y=D2
1510 GOTO 1700
1520 LET Y=D1
1530 GOTO 1700
1540 LET Y=D3
1550 GOTO 1700
1560 LET Y=D6
1570 GOTO 1700
1580 LET Y=D7
1590 GOTO 1700
1600 LET Y=D4
1610 GOTO 1700
1700 GOSUB 2000
1710 NEXT N
1720 GOTO 1260
2000 REM PLOT DATA POINTS
2005 IF E[N]<1 THEN 2080
2010 LET X=85*(.434*LOG(F[N])-2)
2020 LET Y=127.5*(.434*LOG(Y)+2-J8)
2030 IF Y>0 THEN 2050
2040 LET Y=0
2050 IF Y <= 255 THEN 2070
2060 LET Y=255
2070 CALL (43,X,Y,1)
2080 RETURN
3000 CALL (14,M1,0,C8)
3010 LET J=1
3015 GOSUB 3200
3020 CALL (13,Z,C8,S1)
3025 LET J=2
3030 GOSUB 3200
3035 CALL (13,Z,C8,S2)
3040 IF S[31]=-1 THEN 3100
3045 LET S3=S2
3050 LET S4=S1
3055 GOTO 3150
3100 LET J=3
3105 GOSUB 3200
3110 CALL (13,Z,C8,S3)
3115 LET J=4
3120 GOSUB 3200
3125 CALL (13,Z,C8,S4)
3150 LET N=1
3160 LET F[1]=(F[1]+F[M1])/2
3170 GOTO 230
3200 CALL (14,0,0,Z)
3210 FOR N=1 TO M1
3220 LET K=M[N]
3230 CALL (10,D[K,J],Z,Z)
3240 NEXT N
3250 RETURN
9000 CALL (2,F)
9999 END

```

APPENDIX G

Curve Fitting Equation for Bead and Line Trimming

MacKenzie and Sanderson⁽⁵⁾ give a formula for the imaginary part of the impedance at the center of a dielectric bead in a coaxial line as a function of frequency. They use this formula to determine the amount of under and/or overcutting of the line, and beadface compensation necessary to achieve a low VSWR for the bead support. Since they do not give a derivation of this formula, this appendix is devoted to deriving a formula for the reflection coefficient of the bead analogous to their formula for the imaginary part of the impedance.

Figure 15 is a schematic representation for the TEM mode representation for a bead in a coaxial line. The region between and including the step discontinuity capacitances C (Appendix H) is the region in which the bead support resides. The capacitances arise from the step introduced by overcutting of the outer conductor and undercutting the inner conductor to make Z_1 , the characteristic impedance of the line in the bead region, the same as Z_0 , the characteristic impedance of the normal air filled portion of the line. The presence of the additional capacitances C introduces a lumped circuit shunt reactance at the bead faces thus producing a reflection of the TEM wave. In order to offset this additional capacitance and do away with the reflection, some of the dielectric material is removed from the bead faces, i.e., a groove is cut in each face.

The impedance Z_2 is the parallel combination of the capacitance C and the characteristic impedance Z_0 . This impedance will be more fully discussed later in Appendix I.

The impedance Z_3 is Z_2 transformed through the bead region. For the lossless bead

$$Z_3 = Z_1 \left(\frac{Z_2 + j Z_1 \tan \beta l}{Z_1 + j Z_2 \tan \beta l} \right) \quad (G.1)$$

where β is the imaginary part of the propagation constant in the bead, or

$$\beta = \frac{2\pi \epsilon_r^{1/2}}{\lambda}$$

ϵ_r is the real part of the relative dielectric constant, and λ is the free space wavelength. Finally Z is the impedance at the other face of the bead consisting of $1/\omega C$ and Z_3 in parallel, and is supposed to equal Z_0 for reflectionless bead design.

$$Z = \frac{-jXZ_3}{Z_3 - jX} \quad (G.2)$$

where

$$X \equiv 1/\omega C$$

Γ is the reflection coefficient looking to the right into the bead and is given by

$$\Gamma = \frac{Z - Z_0}{Z + Z_0} \quad (G.3)$$

When $-jX$ is expressed in terms of Z_0 and Z_2 this equation can be written in terms of Z_0 , Z_1 , Z_2 , and $\tan \beta l$. Since Z_1 and Z_2 will be close to Z_0 it is convenient to write

$$Z_1 = Z_0 + \delta Z_1 \quad (G.4)$$

and

$$Z_2 = Z_0 + j \delta Z_2$$

where δZ_1 and δZ_2 are small and vanish as the bead and line are trimmed.

When these are substituted into (G.1), and (G.3) is reduced to first order in δZ_1 and δZ_2 , the following expression for the magnitude of Γ results:

$$|\Gamma| = |\delta Z_1 \sin \beta l + \delta Z_2 \cos \beta l| \quad (G.5)$$

where δZ_1 and δZ_2 are the impedances δZ_1 and δZ_2 divided by Z_0 , or the corresponding magnitude of the reflections caused by Z_1 being different from Z_0 , and C being nonzero, respectively.

Using the expression for Z_2 given in Appendix I leads to

$$\delta Z_2 = -\frac{D_2 f}{f_0} \quad (G.6)$$

where

$$\begin{aligned} D_2 &= (D_2)_0 (1 - d/d_0) \\ d_0 &= Z_{02} (D_2)_0 l / 2\pi (Z_{02}^2 - 1) \\ Z_{02} &= (\epsilon_r / \epsilon_{re})^{1/2} \end{aligned}$$

\mathcal{L} is the depth of the compensation cut into the bead faces, \mathcal{L}_0 is the depth of cut for full compensation, $(D_r)_0$ is the measured reflection from the bead faces at f_0 where the bead is one wavelength in length, Z_0 is the desired characteristic impedance (50 ohms), ϵ_r is the relative dielectric constant of the bead material, ϵ_{re} is the effective relative dielectric constant of the bead in the compensated region for which Z_{02} is the normalized characteristic impedance, and \mathcal{L} is the total bead length.

Z_1 is given by

$$Z_1 = \frac{\ln b'/a'}{\epsilon_r^{1/2} \ln b/a} \quad (G.7)$$

where a and b are the inner and outer conductor diameter respectively in the air-filled regions, and a' and b' are the conductor diameters in the bead region that have been chosen to make Z_1 approximately one. If a' and b' have been chosen correctly for the given dielectric constant, then Z_1 will be unity. However, if a' is too large by $\delta a'$ and b' is too large by $\delta b'$, and ϵ_r too large by $\delta \epsilon_r$, that is using

$$\begin{aligned} a' + \delta a' \\ b' + \delta b' \\ \epsilon_r + \delta \epsilon_r \end{aligned} \quad (G.8)$$

then using (G.7) and (G.8) and keeping only first-order terms in $\delta a'/a'$, $\delta b'/b'$ and $\delta \epsilon_r/\epsilon_r$ gives (for the 50 ohm line)

$$\delta Z_1 = \frac{6}{5 \epsilon_r^{1/2}} \left(\frac{\delta b'}{b'} - \frac{\delta a'}{a'} \right) - \frac{1}{2} \frac{\delta \epsilon_r}{\epsilon_r} \quad (G.9)$$

The electrical phase shift βl can be interpreted in the following way⁽⁵⁾:

$$\beta l = \frac{2\pi \epsilon_r^{1/2} l}{\lambda} = \frac{2\pi l_e}{\lambda} = \frac{2\pi f}{f_0} \quad (\text{G.10})$$

where

$$l_e f_0 = v$$

l_e is the electrical length across the bead, v is the speed of light, and f_0 is the frequency for which l_e is one wavelength.

Equation (G.5) can now be rewritten as

$$|\Gamma| = \left| D_1 \sin \frac{2\pi f}{f_0} - \frac{D_2 f}{f_0} \cos \frac{2\pi f}{f_0} \right| \quad (\text{G.11})$$

where

$$D_1 = \frac{6}{5 \epsilon_r^{1/2}} \left(\frac{\delta b'}{b'} - \frac{\delta a'}{a'} \right) - \frac{1}{2} \frac{\delta \epsilon_r}{\epsilon_r}$$

and

$$D_2 = (D_2)_0 (1 - d/d_0)$$

Equation (G.11) is used in the bead and line trimming procedure for obtaining a low reflection coefficient.

APPENDIX H

Step Capacitance

Combining the equations given in Moreno⁽¹¹⁾, the following expression for the step capacitance in picofarads at the uncut face of the bead support results:

$$C = \pi \epsilon_r \left[b \mathcal{C}_1 \left(\frac{b-a}{b-a'}, \frac{b}{a'} \right) + a \mathcal{C}_2 \left(\frac{b-a}{b'-a}, \frac{b'}{a} \right) \right] \quad (\text{H.1})$$

where the first capacitance per unit length \mathcal{C}_1 is given by figure 6-21 in Moreno and the second by figure 6-22. ϵ_r , a , b , a' , and b' are defined in Appendix G. After some of the face material has been removed this capacitance changes to C' , where

$$C > C' > \epsilon_{re} C / \epsilon_r \quad (\text{H.2})$$

and where ϵ_{re} is the effective dielectric constant associated with the compensated part of the bead (Appendix I).

The value for C given by (H.1) should be multiplied by a frequency factor⁽¹¹⁾ when λ , the free space wavelength, becomes an appreciable percentage of $b-a$; and should also be multiplied by a proximity factor⁽¹¹⁾ accounting for interactions between the fringing fields from the step discontinuities when the bead length approaches $b-a$.

APPENDIX I

Effective Dielectric Constant and Face Compensation

In order to nullify the step capacitance and its resultant reflection a toroidal groove is cut into each end face of the bead support. The depth to which this groove is cut is determined by the amount of step capacitance to be nullified, the dielectric constant, and the inner and outer diameter of the toroid.

An exact formula for the compensation depth can only be obtained by a detailed consideration of the interaction between the evanescent modes, the step, and the compensated bead. An investigation of this magnitude is both beyond the scope and needs of this report. Therefore, the following intuitive derivation is presented that gives an order-of-magnitude estimate of the depth. It has proven quite useful and adequate for the purpose of trimming beads.

Figure 16 shows a profile section of one end of the bead support and its equivalent circuit. The compensating toroidal region of length d has an effective dielectric constant ϵ_{re} . \mathcal{C}_0 is the capacitance per unit length in the uncompensated bead region. Through this compensating region of characteristic impedance $Z_{02} (\neq Z_0)$ the TEM wave travels with a propagation constant β . The magnitude of the step capacitance C' lies between C and $\epsilon_{re} C / \epsilon_r$ depending on the dimensions of the toroidal compensating section where C is the step capacitance when $d = 0$ or before any compensation

is effected. The diameters of the various regions are shown in the profile, and are such that

$$\ln b/a = \frac{\ln b'/a'}{\epsilon_r^{1/2}} \quad (\text{I.1})$$

which give a characteristic impedance of Z_0 .

Using the equations given by Cruz⁽⁷⁾ the following relationships can be derived for ϵ_{re} , \mathcal{L}_0 and \mathcal{L} .

$$\epsilon_{re} = \frac{\epsilon_r}{1 + \left(\frac{\epsilon_r - 1}{\epsilon_r^{1/2}} \right) \frac{\ln b''/a''}{\ln b/a}} \quad (\text{I.2})$$

$$\mathcal{L}_0 = \frac{2\pi\epsilon_r\epsilon_0}{\ln b'/a'} \quad (\text{I.3})$$

$$\mathcal{L} = \frac{\epsilon_{re}\mathcal{L}_0}{\epsilon_r} \quad (\text{I.4})$$

where ϵ_0 is the free space dielectric constant.

The impedance Z_L is given by

$$Z_L = Z_0 \left(\frac{Z + j Z_0 \tan \beta l}{Z_0 + j Z \tan \beta l} \right) \quad (\text{I.5})$$

where Z is the parallel combination impedance of C' and Z_0 .

That is,

$$\begin{aligned} Z &= \frac{-j'X Z_0}{Z_0 - j'X} \\ &\approx Z_0 (1 - j'Z_0/X) \end{aligned} \quad (I.6)$$

where

$$X \equiv 1/\omega C'$$

and where ω is the radian frequency. The approximation in equation (I.6) is quite adequate for the present needs.

When equation (I.5) is reduced to first order in Z_0/X the following expressions result:

$$\delta Z_2 = \frac{\frac{(Z_{02}^2 - 1) \tan \beta d}{Z_{02}} - \frac{1}{X}}{1 + j \frac{\tan \beta d}{Z_{02}}} \quad (I.7)$$

where

$$\begin{aligned} Z_2 &\equiv Z_2/Z_0 \approx 1 + j' \delta Z_2 \\ Z_{02} &\equiv Z_{02}/Z_0 = (\epsilon_r/\epsilon_{re})^{1/2} \\ X &\equiv X/Z_0 \\ \beta &= 2\pi \epsilon_{re}^{1/2} / \lambda \end{aligned}$$

where λ is the free space wavelength. Then δZ_2 can be reduced to

$$\delta Z_2 = 2\pi f Z_0 \left[\frac{\epsilon_{re}^{1/2} d}{\nu Z_0} \left(\frac{Z_{02}^2 - 1}{Z_{02}} \right) - C' \right] \quad (I.8)$$

where ν is the free space speed of light and f is the frequency.

The approximation $\tan \beta d \approx \beta d$ has been used in arriving at equation (I.8) and is in keeping with the approximate nature of the derivation. For the experimental work it is convenient to define a measured parameter D_2 which represents the reflection coefficient caused by the uncompensated or partially compensated step capacitance.

$$D_2 \equiv -\frac{f_0}{f} \delta g_2 \quad (I.9)$$

where D_2 is frequency independent.

It has already been stated that the step capacitance C' is a function of the dielectric configuration to the left of the step capacitance in figure 16. From what has been stated in Appendix H it is clear that C' can vary from C given by equation (H.1) for $d=0$, to $\epsilon_r C / \epsilon_r$ when $d=\infty$. There is some depth d_0 where the compensating toroid just nullifies C causing the reflection and D_2 to vanish. It has been found experimentally that C' is given approximately by $C(\epsilon_r \epsilon_r)^{1/2} / \epsilon_r$ when $d=d_0$. That is, the value ϵ_r' of the dielectric constant for C' when the compensation depth is correct (no reflections) is given approximately by the geometric mean of ϵ_r and ϵ_r . Clearly, ϵ_r' varies in some nonlinear fashion as d is varied. However, for the estimate here it is sufficient to assume that ϵ_r' varies linearly from ϵ_r when $d=0$ to $(\epsilon_r \epsilon_r)^{1/2}$ when $d=d_0$. That is

$$\epsilon_r' = \epsilon_r - \left(\frac{\epsilon_r - (\epsilon_r \epsilon_r)^{1/2}}{d_0} \right) d \quad (I.10)$$

When equations (I.8), (I.9), and (I.10) are combined the following approximation for the measured parameter D_z results:

$$D_z = (D_z)_0 (1 - d/d_0) \quad (\text{I.11})$$

$$d_0 = \frac{\epsilon_{02} (D_z)_0 l}{2\pi(\epsilon_{02}^2 - 1)} \quad (\text{I.12})$$

where $(D_z)_0$ is the value of D_z when $d=0$, and l is the total bead length.

APPENDIX J

Higher Mode Bead Resonances

In an unpublished paper⁽¹⁴⁾ Bussey and Beatty show a way to calculate higher mode bead resonances in a coaxial line that is not over or undercut. They have indicated that, in the case of over or undercutting, their simple approach must be modified in three essential ways: 1) the $\beta\lambda$ for the appropriate regions, the uncut and cut region, must be used; 2) some account for the step capacitance due to the cutting must be made; and 3) since the two regions have different dimensions, the characteristic impedances for the higher modes rather than their wave impedances must be used in the impedance transformation formula.

Following is a derivation for the resonant frequencies of the TE modes in a bead where the inner and outer conductors may be under or overcut respectively. The derivation ignores modifications 2 and 3 above, but follows the Bussey and Beatty derivation for the uncut line almost step for step. The only justification offered for this procedure is that it has proven useful in predicting the TE₁₁ resonant frequencies observed in the experiments.

Figure 17 shows a coaxial line in the region of a dielectric bead support. Z_0 and Z_d are the characteristic impedances (taken to be the wave impedances) for the air and dielectric regions of the line respectively. γ_0 and γ_d are the propagation constants of the two regions, ($e^{-\gamma l}$ understood) and λ_{c0} and λ_{cd} are their cutoff wavelengths. The impedance Z is given in terms of Z_s by

$$Z = Z_d \left(\frac{Z_s + Z_d \tanh \gamma_d l/2}{Z_d + Z_s \tanh \gamma_d l/2} \right) \quad (\text{J.1})$$

where

$$Z_d = \frac{j\omega\mu}{\gamma_d}$$

and⁽¹⁴⁾

$$Z_s = \infty \quad \text{for the even cavity modes}$$

$$Z_s = 0 \quad \text{for the odd cavity modes,}$$

ω is the radian frequency; μ is the magnetic permeability of the dielectric bead which is taken to be that of air.

Further,

$$Z_0 = \frac{j\omega\mu}{\gamma_0} \quad (\text{J.2})$$

The propagation constants are given by

$$\gamma_d = \frac{j2\pi(\epsilon_r - \lambda^2/\lambda_d^2)^{1/2}}{\lambda} = j\beta_d \quad (\text{J.3})$$

and

$$\gamma_0 = \frac{2\pi(\lambda^2/\lambda_{co}^2 - 1)^{1/2}}{\lambda}$$

The cutoff wavelengths for the TE_{m1} modes are⁽¹¹⁾

$$\lambda_c = \frac{\pi b(1 + 1/k)}{(1 + k)\chi_{m1}} \quad (\text{J.4})$$

where b is the inside diameter of the outer conductor, k is ratio of the outer conductor inner diameter to the inner conductor outer diameter, and the denominator is obtained either from tables, or graphically (see Appendix K).

The condition for resonance is taken to be ⁽¹⁴⁾

$$Z = Z_o^* \quad (J.5)$$

where the star signifies complex conjugate. This condition leads to the following conditions for resonance

$$\tan \beta_o l / 2 = \begin{cases} - \left(\frac{\epsilon_r - \lambda^2 / \lambda_{cd}^2}{\lambda^2 / \lambda_{co}^2 - 1} \right)^{1/2} & \text{for the odd modes} \\ \left(\frac{\lambda^2 / \lambda_{co}^2 - 1}{\epsilon_r - \lambda^2 / \lambda_{cd}^2} \right)^{1/2} & \text{for the even modes} \end{cases} \quad (J.6)$$

After a compensation cut into the bead faces has been made, l is taken to be the length of the uncut portion of the bead between the bead faces.

APPENDIX K

TE₁₁ Cutoff Wavelengths

The cutoff wavelengths for the higher TE₁₁ modes in a coaxial line are given by equation (J.4) of Appendix J. The denominator of that expression for the TE₁₁ mode can be obtained from figure 18 which is a graph of the denominator as a function of k . χ'_{11} is a root of

$$J_1'(\chi) N_1'(k\chi) - J_1'(k\chi) N_1'(\chi) = 0 \quad (K.1)$$

for a given value of k . J and N are Bessel functions of the first and second kinds respectively. A table of values for x as a function of k extensive enough for the present investigations was not found. Therefore a simple graphical technique⁽¹⁵⁾ which only requires evaluating the ratio $J_1'(\chi) / N_1'(\chi)$ was employed to find the needed roots. This technique considerably reduces the effort in finding x for equation (K.1), and provides sufficient accuracy for the needs explained in Appendix I.

APPENDIX L

Termination Design Equations

The resistance of a truncated cone of semi-angle θ (figure 12) and ρ surface resistivity is given in the paper by Woods⁽⁸⁾ as

$$R = \frac{\rho \ln b/a}{2\pi \sin \theta} \quad (\text{L.1})$$

which reduces to the familiar equation

$$Z = \frac{Z_m \ln b/a}{2\pi} \quad (\text{L.2})$$

where Z is the wave impedance of the medium.

Since the main field penetrates the film and sets up auxiliary fields within the substrate, there are interactions which take place. The resulting second order effects are handled by the following (figure 12)

$$\frac{b}{b'} = 1 + \frac{\epsilon_r \sin^2 \theta}{4} \quad (\text{L.3})$$

and

$$\frac{b}{b'} = \frac{a}{a'} \quad (\text{L.4})$$

5. REFERENCES

- (1) Daywitt, W. C., Foote, W. J., Campbell, E., "WR15 Thermal Noise Standard," NBS Technical Note 615, issued March 1972.
- (2) Cohn, S. B., Kelly, K. C., "Microwave Measurement of High-Dielectric Constant Materials," IEEE Trans. on MTT, Vol. MTT-14, No. 9, Sept. 1966.
- (3,4) Bussey, H. E., Private Communication, National Bureau of Standards, Boulder, Colorado.
- (5) MacKenzie, T. E., Sanderson, A. E., "Some Fundamental Design Principles for the Development of Precision Coaxial Standards and Components," IEEE Trans. on MTT, Vol. MTT-14, No. 1, Jan. 1966.
- (6) Whinnery, J. R., Jamison, H. W., Robbins, T. E., "Coaxial Line Discontinuities," Proc. IRE, Nov. 1944.
- (7) Cruz, J. E., "Experimental Verification of an Equation for Determining the Effective Dielectric Constant of Center Conductor Supports in Coaxial Transmission Lines," unpublished, NBS Report, March 1966.
- (8) Woods, D., "Improvements in Precision Coaxial Resistor Design," IRE Trans. on Inst., pp. 305-309, Dec. 1962.
- (9) Harris, I. A., "The Theory and Design of Coaxial Mounts for the Frequency Band 0-4000 mc/s," Proc. IEE, Vol. 103C, Monograph No. 132R, pp. 1-20, May 1955.

- (10) Nelson, R. E., Coryell, M. R., "Electrical Parameters of Precision, Coaxial, Air-Dielectric Transmission Lines," National Bureau of Standards Monograph 96, issued June 30, 1966.
- (11) Moreno, T., "Microwave Transmission Design Data," Dover Publications Inc., New York, 1958.
- (12) Sucher, M., Fox, J., Eds. "Handbook of Microwave Measurements," Third Edition, Vol. II, Chapter IX, Polytechnic Press, New York, 1963.
- (13) Holley, A., Private Communication, Hughes Aircraft Company.
- (14) Bussey, H. E., Beatty, R. W., "Higher Mode Resonances of Dielectric Support Beads in Coaxial Lines," unpublished, NBS Report, June 1966.
- (15) Truell, R., "Concerning the Roots of $J_n'(x)N_n'(kx) - J_n'(kx)N_n'(x) = 0$," J. of Appl. Phys., Vol. 14, p. 350, July 1943.

U.S. DEPT. OF COMM. BIBLIOGRAPHIC DATA SHEET	1. PUBLICATION OR REPORT NO. NBSIR 73-334	2. Gov't Accession No.	3. Recipient's Accession No.
4. TITLE AND SUBTITLE A Broadband Coaxial Noise Source Preliminary Investigations		5. Publication Date October 1973	6. Performing Organization Code
		8. Performing Organization	
7. AUTHOR(S) W. C. Daywitt and L. D. Driver		10. Project/Task/Work Unit No. 2726449	
9. PERFORMING ORGANIZATION NAME AND ADDRESS NATIONAL BUREAU OF STANDARDS, Boulder Labs. DEPARTMENT OF COMMERCE Boulder, CO 80302		11. Contract/Grant No. CCG/Navy Blanket Program 73-78	
		13. Type of Report & Period Covered Interim Status Report - FY 73	
12. Sponsoring Organization Name and Address Department of Defense, Calibration Coordination Group Attn: Melvin L. Fruechtenicht, Chairman Army Metrology and Calibration Center, Redstone Arsenal Huntsville, Alabama 35809		14. Sponsoring Agency Code	
		15. SUPPLEMENTARY NOTES	
16. ABSTRACT (A 200-word or less factual summary of most significant information. If document includes a significant bibliography or literature survey, mention it here.) <p>This report describes investigations that were performed in fiscal year 1973, by the Noise and Interference Section of the Electromagnetics Division of the Institute for Basic Standards of the National Bureau of Standards preliminary to the design and construction of a coaxial thermal noise source in fiscal year 1974. The intent is to develop a coaxial thermal reference noise source that will operate at nominally 1000°C and will have a low reflection coefficient from 0.1 to 12 GHz.</p>			
17. KEY WORDS (Alphabetical order, separated by semicolons) Bead support; noise standard; resistive termination.			
18. AVAILABILITY STATEMENT <input type="checkbox"/> UNLIMITED. <input checked="" type="checkbox"/> FOR OFFICIAL DISTRIBUTION. DO NOT RELEASE TO NTIS.		19. SECURITY CLASS (THIS REPORT) UNCLASSIFIED	21. NO. OF PAGES
		20. SECURITY CLASS (THIS PAGE) UNCLASSIFIED	22. Price

